APR 1979

NASA Contractor Report 3111

COMPLETED
ORIGINAL

An Analytical Investigation of the Performance of Solar Collectors as Nighttime Heat Radiators in Airconditioning Cycles

Clay B. Jones and Frederick O. Smetana

CONTRACT NAS1-14208
MARCH 1979

NASA

64

NASA Contractor Report 3111

An Analytical Investigation of the Performance of Solar Collectors as Nighttime Heat Radiators in Airconditioning Cycles

Blank Page

Clay B. Jones and Frederick O. Smetana
North Carolina Science and Technology Research Center
Research Triangle Park, North Carolina

Prepared for
Langley Research Center
under Contract NAS1-14208

NASA
National Aeronautics
and Space Administration

Scientific and Technical
Information Office

1979

Blank Page

TABLE OF CONTENTS

	Page
NOMENCLATURE	v
SUMMARY	1
INTRODUCTION	2
COOLING MODE ANALYSIS	4
RESULTS OF COOLING MODE ANALYSIS	21
CONCLUSION	41
BIBLIOGRAPHY	43
APPENDIX	44

Blank Page

Blank Page

NOMENCLATURE

A_c	Collector area, m^2
C_p	Specific heat coefficient, $\frac{J}{Kg\ K}$
COP	Coefficient of performance, dimensionless
COP_h	Heating mode COP
COP_c	Cooling mode COP
d	Distance between collector plate and cover, m
d_1	d for gap 1
d_2	d for gap 2
g	Acceleration due to gravity, m/sec^2
g_x	g in the "x" direction
h_i, i = 1 - 4	Enthalpy of refrigerant at various points in the cycle, KJ/Kg
$h_{c,p-s}$	Convection heat transfer coefficient, collector plate to surroundings, $W/m^2\ K$
$h_{c,p-c}$	Convection heat transfer coefficient, collector plate to cover, $W/m^2\ K$
k	Thermal conductivity of air, W/m K
$\dot{m}_1$	Mass flow rate through gap 1, Kg/sec
$\dot{m}_2$	Mass flow rate through gap 2, Kg/sec
Nu	Nusselt number, dimensionless
P	Pressure, Bars
P_a	Atmospheric pressure, Bars (1 bar = 10^5 Pa)
$Q_{gap\ 1}$	Net heat dissipated through gap 1, W

$Q_{gap\ 2}$	Net heat dissipated through gap 2, W
$q_{gap\ 1}$	Heat dissipated through gap 1 per unit area of collector, W/m^2
$q_{gap\ 2}$	Heat dissipated through gap 2 per unit area of collector, W/m^2
$q_{tot\ i}$, i = 1 - 4	Heat dissipated from collector geometry "i" per unit area of collector, W/m^2
$q_{r,p-s}$	Radiation heat transfer from the collector plate to the sky, W/m^2
$q_{c,p-c}$	Convection heat transfer from the collector plate to the cover, W/m^2
$q_{c,p-s}$	Convection heat transfer from the collector plate to the surroundings, W/m^2
$q_{c,c-s}$	Convection heat transfer from the cover to the surroundings, W/m^2
$q_{r,c-s}$	Radiation heat transfer from the cover to the sky, W/m^2
$q_{r,p-c}$	Radiation heat transfer from the collector plate to the cover, W/m^2
R	Gas constant for air, $\frac{J}{Kg\ K}$
Ra	Rayleigh number, dimensionless
T	Temperature, K
T_i, i = 1 - 3	Temperature at various points in the cycle, K
T_a	Ambient temperature, K
T_c	Cover temperature, K
T_p	Collector plate temperature, K
T_s	Effective black-body sky temperature, K
T_{01}	Bulk fluid temperature at exit of gap 1, K

T_{02}	Bulk fluid temperature to exit of gap 2, K
T_{g1}	Air temperature across gap 1, K
T_{g2}	Air temperature across gap 2, K
u	Velocity in the "x" direction, m/sec
u_1	Velocity in the "x" direction through gap 1, m/sec
u_2	Velocity in the "x" direction through gap 2, m/sec
$\bar{u}$	Mean air velocity in the "x" direction, m/sec
$\bar{u}_1$	$\bar{u}$ for gap 1, m/sec
$\bar{u}_2$	$\bar{u}$ for gap 2, m/sec
V	Wind speed, m/sec
v	Velocity in the "y" direction, m/sec
W	Collector width, m
x	Direction along the plate
y	Direction perpendicular to the "x" direction
α	Molecular thermal diffusivity, m^2/sec
β	Volume coefficient of expansion 1/ K
ΔT	Temperature difference, K
ε_p	Collector plate emittance, dimensionless
ε_c	Cover emittance, dimensionless
ϑ	Collector tilt angle, degrees
μ	Dynamic viscosity, N sec/m^2
ν	Kinematic viscosity, m^2/sec
ρ	Density, $\frac{Kg}{m^3}$
ρ_a	Atmospheric density

ρ_o	Density at bulk fluid temperature, $\frac{Kg}{m^3}$
σ	Stefan-Boltzmann constant, $\frac{W}{m^2\ {}^oK}$

SUMMARY

An analytical investigation was carried out to determine the ability of typical solar collectors to serve as nighttime heat radiators. Such use might be made of the collectors during the summertime where they then serve as the condenser in a heat pump cycle with eiectrically-driven mechanical compressor. In winter the collectors form a solar-heated evaporator in the heat pump cycle. It was found that if one opens the upper and lower ends of a collector, large free convection currents may be set up between the collector surface and the cover glass(es) which can result in appreciable heat rejection. If the collector is so designed that both plate surfaces are exposed to convection currents when the upper and lower ends of the collector enclosure are opened, the heat rejection rate is 300 watts/m^2 when the plate is 13^{o}C above ambient. This is sufficient to permit a collector array designed to provide 100% of the heating needs of a home to reject the accumulated daily air conditioning load during the course of a summer night. This also permits the overall energy requirement for cooling to be reduced by at least 15% and shift the load on the utility entirely to the nighttime hours.

INTRODUCTION

Using solar collectors as heat sources in heat pump cycles is a concept that has received favorable consideration from several designers of solar energy utilization systems. The corollary concept — using the solar collectors as nighttime radiations in heat pump cooling cycles — is scarcely mentioned. It is evident, however, that some beneficial summertime use should be made of the solar collectors in such heating systems in order to help justify their large capital cost. Three uses come quickly to mind: a heat source for an absorption chiller; a source of domestic hot water; a heat source in a Rankine cycle power unit.

The first use requires an extensive summer-winter changeover to utilize the collectors efficiently in the winter. If one is willing to sacrifice efficiency however, the collectors can be used for direct heating (non-heat pump) in the winter with very little additional capital cost over that for an absorption chiller. Such systems have been built and tested at several locations.

The second use is an obvious one, but it is readily shown that the collector area needed for winter heating is much greater than that needed for summertime domestic hot water production. This is therefore not an effective use of the collectors. The Rankine cycle power unit could employ the collectors in a system to supply part of the building's electrical power needs in the summer, or it could drive a mechanical chiller instead.

Systems have been built and operated successfully for both applications. With presently-available technology the capital costs of a Rankine cycle power unit are quite high because the expander particularly and the condensate pump to a limited extent represent custom hardware that must be <u>designed</u> and fabricated for specific conditions in specific

installations. Addition of a Rankine cycle power unit would add about 70% to the cost of the solar-assisted heat pump.

For these reasons a less capital-intensive use for the collectors in the summertime was sought. It was recognized that such a use would probably not save as much fossil fuel energy as a more capital-intensive use, but it would probably be less difficult to maintain and more suited to individual residential applications.

Since the solar assisted heatpump concept really implies the concurrent use of large scale thermal storage so as to provide heat at night, on cloudy days, or for periods when the mechanical compressor cannot be operated, it was felt that the entire cycle could easily and inexpensively be shifted from the daytime heating mode in winter to the nighttime chilling mode in summer. Under these conditions the solar collectors become the freon condenser instead of the freon evaporator as when the system is in the heating mode. The advantages of such operation are:

1. The system draws power from the utility at off-peak times (sunset-to-sunrise).

2. The system COP is higher for nighttime operation than for daytime operation because condensing temperatures may be 6-30^{o}C lower.

It is conservatively estimated that because of these factors the power cost for rejecting a given amount of heat can be reduced by at least 15% compared with a conventional air conditioning system without large-scale thermal storage. This estimate is based on the assumption that the solar collector area needed for winter heating will in fact be sufficient to reject all the heat necessary for summer chilling while remaining only slightly above ambient temperature.

It was to investigate the validity of that assumption that the following analytical study was carried out.

COOLING MODE ANALYSIS

An investigation into the heat transfer characteristics of four collector geometries was carried out in an effort to establish probable performance for solar collectors operating as nighttime radiators. The collector geometries considered were:

(1) Flat plate with cover system removed (No Cover).

(2) Flat plate with one cover (Closed Cover).

(3) Flat plate with one cover and an opening between the plate and the cover at the top and bottom of the collector (Open End 1).

(4) Flat plate with one cover and an opening between the plate and cover and between the plate and back insulation at the top and bottom of the collector (Open End 2).

Selection of the collector geometries stated above stems from a desire to utilize a collector that will perform well both as a heat absorber and as a heat rejecter without requiring extensive seasonal modifications. Complete removal of the cover system during the summer is the most desirable solution from a heat transfer standpoint, but was deemed impractical on any but very small installations. One might suggest the use of a jalousie window cover system which could be opened during the summer and closed during the winter months. However, such an arrangement probably increases costs to the point of overcoming the collector cost advantages afforded by the heat pump concept. Additionally, wind loads, mechanical complexity, and increased weight pose difficulties for a scheme of this type.

Consideration of these problems associated with cover system removal suggests the need for a collector that can effectively dissipate heat with the cover system in place. Collector geometries (3) and (4) above are presented as a possible means of fulfilling this requirement without compromising heating mode performance or requiring undue mechanical complexity and additional construction costs. In both configurations the collector box sides at the top and bottom of the collector are hinged so that they can be opened to allow air flow across the collector plate. Geometry (3) employs a conventional collector arrangement with the back insulation adjacent to the plate (see Figure 1). In geometry (4) the collector plate is supported by standoffs to allow flow on both sides of the plate (see Figure 2). It was felt that by taking advantage of the expected free convection draft or "chimney effect" these types of collectors may possess adequate heat dissipation abilities.

Cooling mode operation requires that the collector subsystem function as the refrigerant condenser, rejecting heat to the atmosphere. This heat transfer is accomplished by means of convection to the surrounding air at ambient temperature and radiation from the collector to the night sky. The effectiveness of both of these modes of heat exchange is very difficult to predict in that they are influenced by such highly variable parameters as wind speed, ambient temperature, atmospheric humidity, and cloudiness. However, it was felt that reasonable operating limits could be obtained by assuming low wind speeds coupled with very clear and very cloudy sky conditions. In addition to these restrictions, the following assumptions were made to simplify the heat transfer analysis:

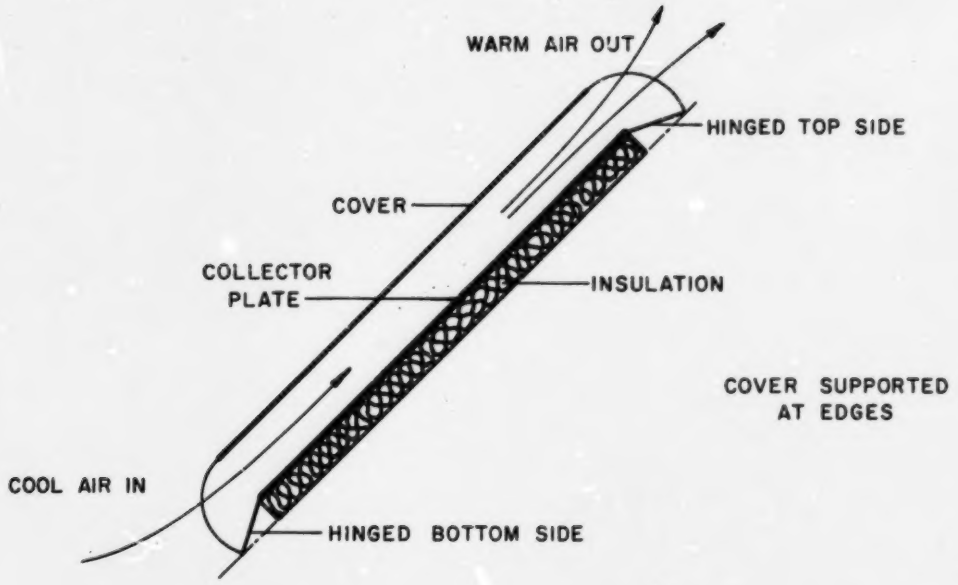

FIGURE 1. Detail of Collector Geometry 3.

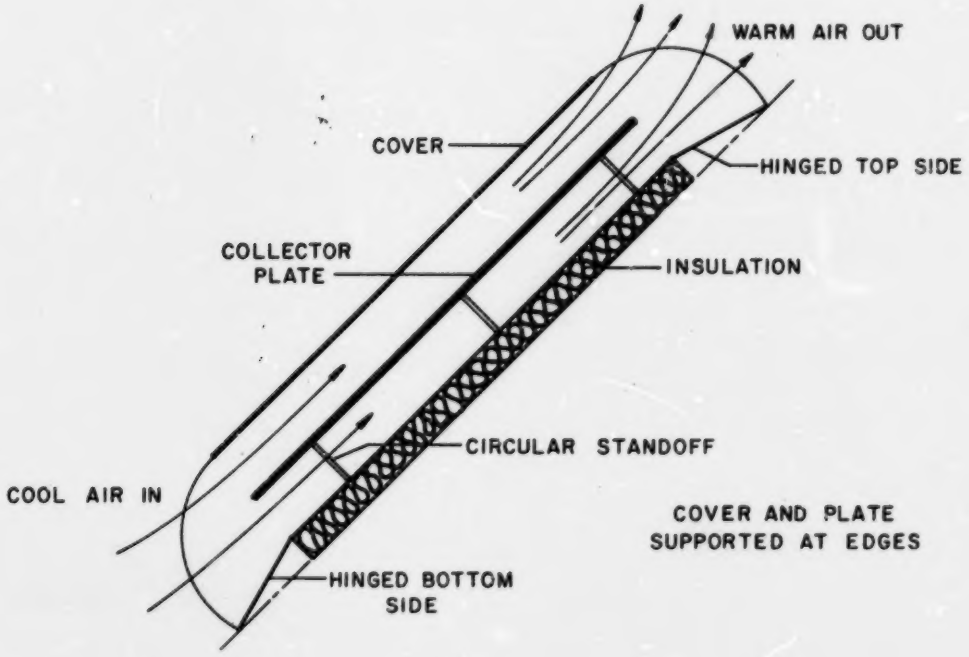

FIGURE 2. Detail of Collector Geometry 4.

(1) The system operation is steady state. That is, there are no time-dependent variables.

(2) The absorber plate and the cover are at some average temperature.

(3) Edge and bottom heat losses are negligible.

(4) Thermal capacity effects of the collector plate and cover are negligible.

(5) There is negligible temperature drop across the cover.

(6) The cover is opaque to longwave radiation (the cover blocks direct radiation from the plate to the sky - a good approximation for glass).

(7) Back radiation from the night sky approximates that of a black-body at some effective sky temperature.

(8) Radiation characteristics of the plate and cover are considered independent of wavelength (gray-body assumption).

The appropriate value for the effective sky temperature for various atmospheric conditions appears to be somewhat in doubt. For a fairly clear night sky Hackforth [2] suggest 273 K, while Kreith recommends a value of 227 K. For very cloudy sky conditions a value equal to the ambient temperature at the ground would seem realistic. In an effort to establish suitable limits, these effective sky temperatures are considered in combination with wind speeds of 0, 2, and 5 meters per second.

Results of the analysis for the various geometries operating under the conditions stated above are presented graphically in terms of the heat dissipation rate as a function of the difference between the collector plate temperature and the ambient temperature (ΔT). Additionally, the effect of wind speed and the effective sky temperature at a ΔT of $15^{\circ}C$ is considered. Major elements of the heat transfer analysis for the collector geometries are presented in the following sections while a more detailed treatment for open-ended collectors is given in the Appendix.

1. Flat Plate with Cover System Removed (No Cover) (Figure 3)

The flat plate with no cover system is the most effective heat dissipator of the geometries considered. Additionally, it is the easiest to treat analytically, the heat transfer being composed of direct radiation from the collector plate to the sky and convection from the plate to the surrounding air at ambient temperature. Thus,

$$q_{tot\ 1} = q_{r,p-s} + q_{c,p-s} \tag{1}$$

where

$q_{tot\ 1}$ = total heat flux per unit area of collector

$q_{r,p-s}$ = radiative heat flux component

$q_{c,p-s}$ = convective heat flux component

If the radiation properties of the collector plate are assumed independent of wavelength (gray), the radiative heat exchange between the sky (a black-body) and the plate may be found from the simple expression,

$$q_{r,p-s} = \varepsilon_p \sigma(T_p^4 - T_s^4) \quad (W/m^2) \tag{2}$$

where

ε_p = surface emittence of the collector plate

σ = Stefan-Boltzmann constant (W/m^2 K)

T_s = effective sky temperature (K)

T_p = average collector plate temperature (K)

The convective heat transfer from the plate to the surrounding air may be found from the following dimensional expression for the heat transfer coefficient recommended by Duffie and Beckman and by Meinel:

$$h_{c,p-s} = (5.7 + 3.8\ V) \tag{3}$$

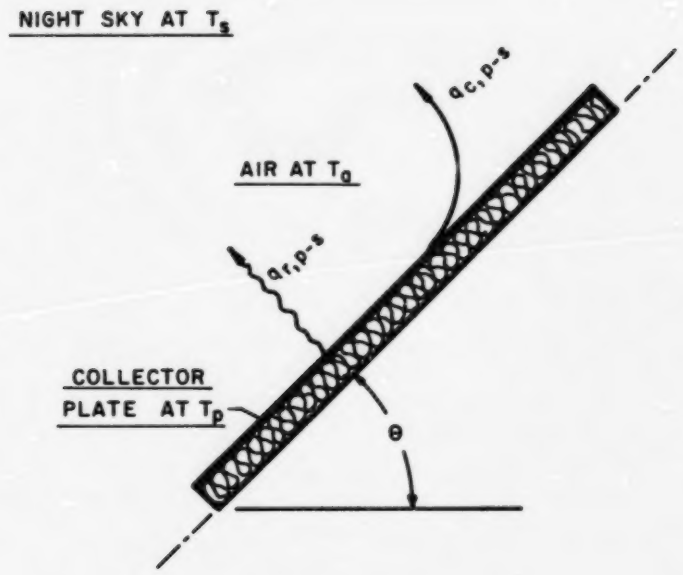

FIGURE 3. Heat Transfer Components in No-Cover Collector.

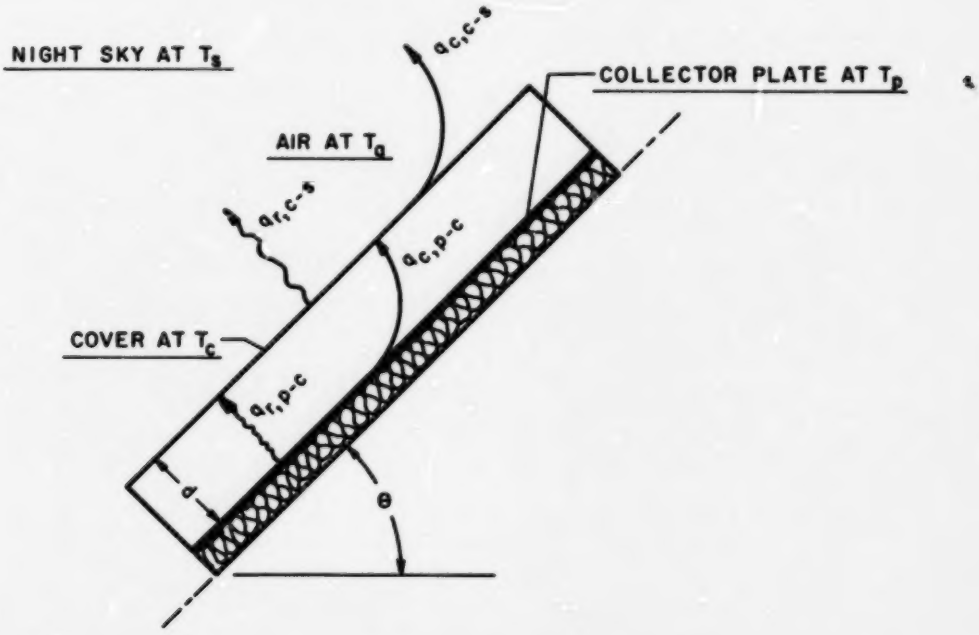

FIGURE 4. Heat Transfer Components in Closed-Cover Collector.

where

$h_{c,p-s}$ = convective heat transfer coefficient (W/m^2 K)

V = wind speed (m/sec)

Thus, the convective heat transfer component ($q_{c,p-s}$) is given by

$$q_{c,p-s} = (5.7 + 3.8\ V)\ (T_p - T_a) \quad (W/m^2) \tag{4}$$

where

T_a = ambient temperature (K)

Thus, the total heat transferred per unit area ($q_{tot\ 1}$) for the flat plate with no cover may be expressed in the following form:

$$q_{tot\ 1} = \varepsilon_p\ \sigma(T_p^4 - T_s^4) + (5.7 + 3.8\ V)\ (T_p - T_a) \quad (W/m^2) \tag{5}$$

2. Flat Plate with One Cover (Closed Cover) (Figure 4)

The heat loss components (neglecting edge and bottom loses) from a collector with one glass cover are shown in Figure 4. Heat exchange from the collector plate to the cover takes place through radiation and free convection heat transfer generated by the temperature gradient between the parallel planes. Assuming no direct radiation from the collector plate to the sky, the net heat transfer from the closed cover collector ($q_{tot\ 2}$) is the heat dissipated from the cover to the night sky and surrounding air, the characteristics of which are as treated in the previous section. Thus,

$$q_{tot\ 2} = \varepsilon_c\ \sigma(T_c^4 - T_s^4) + (5.7 + 3.8\ V)\ (T_c - T_a) \quad (W/m^2) \tag{6}$$

where

ε_c = surface emittance of the cover

T_c = average cover temperature (K)

The unknown cover temperature (T_c) may be found by performing a heat balance on the cover as follows:

$$q_{c,p-c} + q_{r,p-c} = q_{tot\ 2} \tag{7}$$

where

$q_{c,p-c}$ = convective heat transfer from the collector plate to the cover (W/m^2)

$q_{r,p-c}$ = radiative heat transfer from the collector plate to the cover (W/m^2)

The radiation component for gray-body parallel planes is given by:

$$q_{r,p-c} = \frac{\sigma(T_p^4 - T_c^4)}{\frac{1}{\varepsilon_c} + \frac{1}{\varepsilon_p} - 1} \tag{8}$$

The convective component is given by:

$$q_{c,p-c} = h_{c,p-c}(T_p - T_c) \tag{9}$$

where

$h_{c,p-c}$ = convection heat transfer coefficient (W/m^2 K)

Determination of the convective heat transfer coefficient between the plate and cover has been the object of several studies, the most cited of which is by Tabor, presented in 1958. However, a more recent work by Hollands, et al. presents a correlation for calculating Nusselt numbers for inclined, enclosed air spaces of high aspect ratio, having $0 \leq \theta \leq 60$ degrees and $0 \leq Ra \leq 10^5$, where θ is the tilt angle and Ra is the Rayleigh number. This correlation is a closed form expression which has the obvious advantage of suitability for the digital calculations used in this analysis. The equation is as follows:

$$Nu = 1 + 1.44\left[1 - \frac{1708}{Ra \cos\theta}\right]^{*}\left(1 - \frac{(\sin 1.8\ )^{1.6}\ 1708}{Ra \cos}\right) + \left[\left(\frac{Ra \cos\theta}{5830}\right)^{\frac{1}{3}} - 1\right]^{*}$$

$$\theta \leq 60 \text{ degrees} \qquad (10)$$

where

$$Nu = \frac{h_{c,p-c}\ d}{k} \qquad (11)$$

$$Ra = \left(\frac{g\ \beta\ \rho^2\ C_p}{k\mu}\right)\left((T_p - T_c)\ d^3\right) \qquad (12)$$

d = distance between the plate and cover

k = thermal conductivity of the air

g = acceleration due to gravity

ρ = density of air

C_p = specific heat of air

β = coefficient of thermal expansion of air

and

μ = dynamic viscosity of air

Thus, with the use of the expressions given above, the cover temperature (T_c) may be determined through an iterative process for given values of the collector plate temperature (T_p), the ambient temperature (T_a), and the effective sky temperature (T_s). The total heat dissipation rate for the closed cover collector may then be found from equation (6).

3. Flat Plate with One Cover and an Opening Between the Plate and Cover at the Top and Bottom of the Collector (Open End 1 - Figure 5)

In addition to the radiative and convective heat transfer considered

---

NOTE: Starred (*) brackets go to zero when negative.

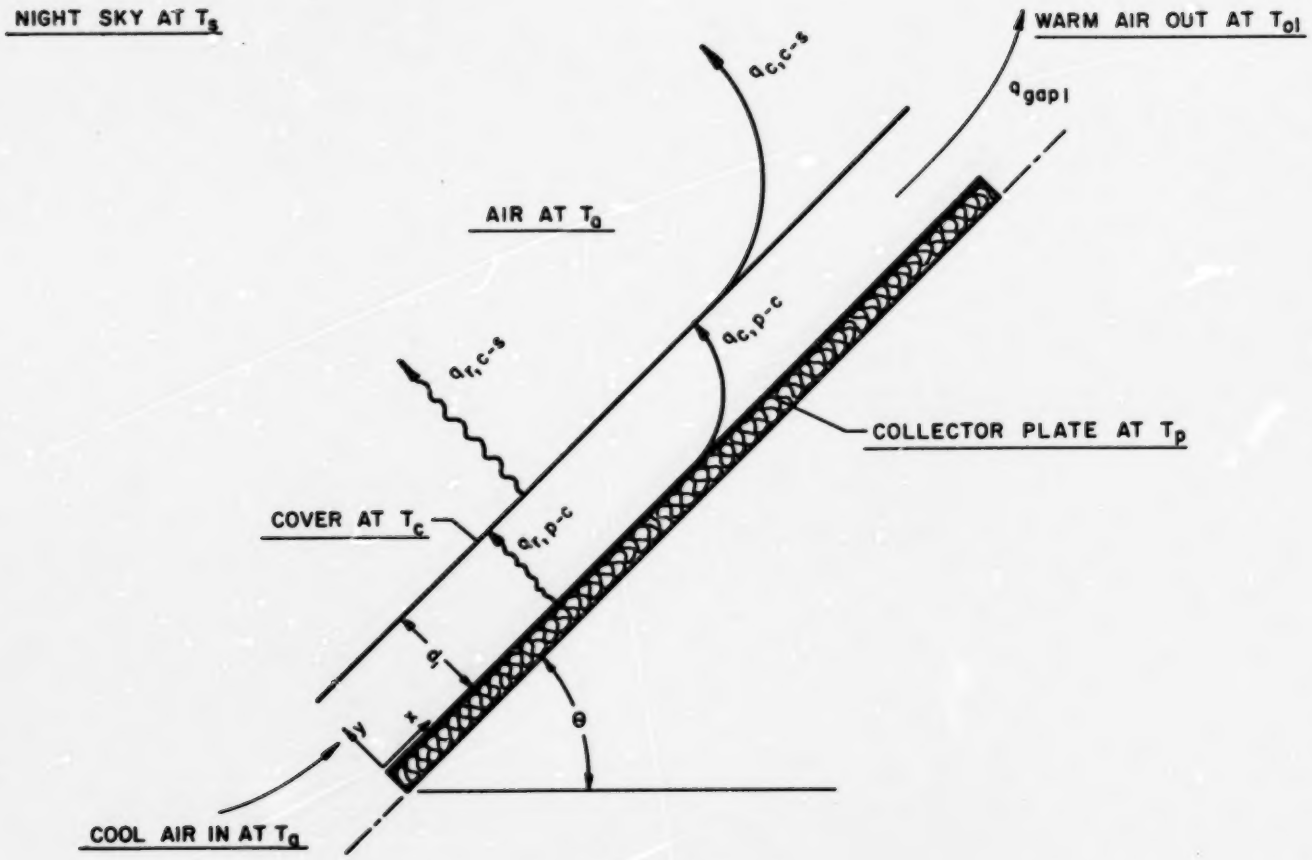

FIGURE 5. Heat Transfer Components in Open-End 1 Collector.

In the previous section, the analysis of this collector geometry is complicated by the natural convection flow through the air gap between the plate and cover producing a draft or "chimney effect" as shown in Figure 5. Air at ambient temperature enters the gap, is heated by the warm collector plate, which produces a buoyant force, thus causing the air to rise until it exits at the top.

If it is assumed that the flow is laminar over the entire length of the plate and that the gap is small compared to the plate length, then it seems reasonable to assume that the velocity and temperature profiles are fully developed at the exit. Additionally, if the profiles are considered to be essentially constant the momentum and energy equations may be solved exactly for the velocity and temperature profiles at the exit.

With a knowledge of these relationships, a mass flow rate and a bulk air temperature at the exit may be calculated from which the energy absorbed by the air may be found. Letting "x" be the direction along the plate, the governing equations for two dimensional, incompressible flow are as follows:

a) Continuity Equation

$$\frac{\partial u}{\partial x} + \frac{\partial v}{\partial y} = 0 \tag{13}$$

b) X-Momentum Equation

$$\rho\left(u \frac{\partial u}{\partial x} + v \frac{\partial u}{\partial y}\right) = - \frac{\partial P}{\partial x} - \rho g_x + \mu \frac{\partial^2 u}{\partial y^2} \tag{14}$$

and c) Energy Equation

$$u \frac{\partial T}{\partial x} + v \frac{\partial T}{\partial y} = \alpha \frac{\partial^2 T}{\partial y^2} \tag{15}$$

where

x = direction along collector plate

y = direction across the air gap

u = velocity in the x direction

v = velocity in the y direction

ρg_x = body force in x direction

ρ = air density[1]

$\frac{\partial P}{\partial x}$ = pressure gradient in the x direction

g_x = acceleration of gravity in the x direction

μ = viscosity (assumed constant)

and

α = molecular thermal diffusivity

Solution of these equations subject to the stated assumptions (see Appendix yields the following results:

Velocity Profile

$$u_1 = \frac{g \sin \theta}{\nu T_a} (T_c - T_o)\left[\frac{yd}{6} - \frac{y^3}{6d}\right] + (T_p - T_a)\left[\frac{yd}{2} - \frac{y^2}{2}\right] \qquad (16)$$

where

ν = kinematic viscosity

Temperature Profile

$$T_{g1} = \frac{y}{d}[T_c - T_p] + T_p \qquad (17)$$

---

[1]The density (ρ) in the body force term is considered to vary with temperature while the density appearing elsewhere is assumed to be constant.

Bulk Fluid Temperature (T_{01}) at Exit

$$T_{01} = \frac{\frac{8}{15}(T_p + T_c)^2 - T_a(T_p + T_c) - \frac{2}{15} T_p T_c}{T_p - 2 T_a + T_c} \quad (18)$$

Mass Flow Through Air Gap ($\dot{m}_1$)

$$\dot{m}_1 = \frac{P_a W d^3 g \sin\theta}{R T_{01} 24 \nu T_a} (T_p - 2 T_a + T_c) \quad (19)$$

where

P_a = atmospheric pressure

W = collector width

R = gas constant for air

The net convective heat transfer from the collector plate to the air flowing through the gap ($Q_{gap\ 1}$) is given by:

$$Q_{gap\ 1} = (\dot{m}_1)(C_p)(T_o - T_a) \quad (W) \quad (20)$$

and

$$q_{gap\ 1} = \frac{1}{A_c} (\dot{m}_1)(C_p)(T_o - T_a) \quad (W/m^2)(\text{unit area}) \quad (21)$$

where

A_c = collector area

The total heat loss ($q_{tot\ 3}$) from the open ended 1 collector is given by:

$$q_{tot\ 3} = q_{gap\ 1} + q_{r,c-s} + q_{c,c-s} \quad (W/m^2) \quad (22)$$

where the heat transfer components from the cover to the sky are as given for the closed cover geometry. Again the solution is dependent on a knowledge of the cover temperature (T_c) which may be found from the appropriate energy balance as before. That is,

$$q_{r,p-c} + q_{c,p-c} = q_{r,c-s} + q_{c,c-s} \tag{23}$$

where

$q_{r,p-c}$ = radiation from plate to cover

$$= \frac{\sigma(T_p^4 - T_c^4)}{\frac{1}{\varepsilon_p} + \frac{1}{\varepsilon_c} - 1} \qquad (W/m^2) \tag{24}$$

$q_{r,c-s}$ = radiation from cover to sky

$$= \varepsilon_c \, \sigma(T_c^4 - T_s^4) \qquad (W/m^2) \tag{25}$$

$q_{c,c-s}$ = convection from cover to surrounding air

$$= (5.7 + 3.8 \, V) \, (T_c - T_a) \qquad (W/m^2) \tag{26}$$

and

$q_{c,p-c}$ = convection from plate to cover

Determination of the convective heat transfer from the collector plate to the cover poses a problem due to the difficulty of obtaining a solution of the governing equations all along the collector length. However the flow is assumed fully developed at the exit (v = 0) and in this region heat is transferred from the collector plate to the cover by pure conduction through the air gap.

Since there is no knowledge of the entrance region flow characteristics, it is assumed that the heat convected from the plate to the cover is of the same order of magnitude all along the length of the collector as it is at the exit. This simplification yields the following result:

$$q_{c,p-c} = \frac{k}{d} (T_p - T_c) \qquad (W/m^2) \tag{27}$$

The cover temperature (T_c) must again be found through an iterative process using the expressions given above and the total heat dissipation

rate for the open ended (1) collector geometry may then be found from equation (22).

4. Flat Plate with One Cover and an Opening Between the Collector Plate and Cover and Between the Plate and Back Insulation at the Top and Bottom of the Collector (Open End 2 - Figure 6)

Analysis of the open-ended 2 collector scheme is essentially as given for open end 1 collector with the addition of the free convection flow on the bottom side of the collector plate. That is,

$$q_{tot\ 4} = q_{tot\ 3} + q_{gap\ 2} \tag{28}$$

where

$q_{tot\ 4}$ = total heat transfer rate for geometry (4)

and

$q_{gap\ 2}$ = convective heat dissipated through the air gap below the collector plate

Fully developed flow at the exit is again assumed. Letting "x" be the direction along the plate and "y" across the air gap, the governing equations are identical to equations (13), (14), and (15).

Solution to these equations subject to the appropriate boundary conditions yields the following results

$$u_2 = \frac{g \sin\theta}{2\nu}\left(1 - \frac{T_p}{T_a}\right)(y^2 - d_2\, y) \tag{29}$$

$$T_{g2} = T_p \tag{30}$$

$$T_{02} = T_p \tag{31}$$

$$\dot{m}_2 = \frac{P\, d_2^3\, W\, g \sin\theta}{12\, R\, \nu}\left(\frac{1}{T_a} - \frac{1}{T_p}\right) \tag{32}$$

where subscript 2 refers to the lower air gap. Thus, $q_{gap\ 2}$ becomes

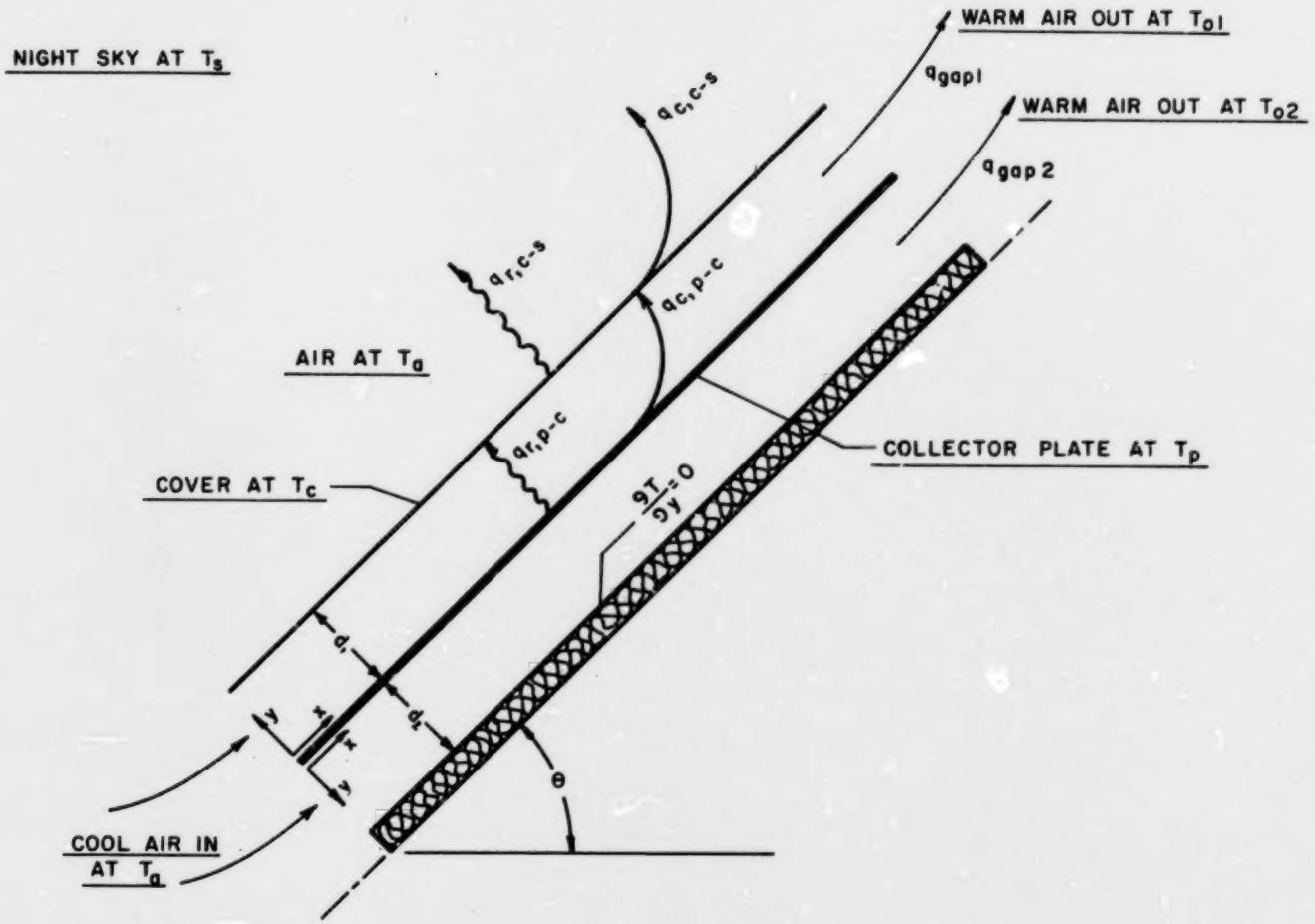

FIGURE 6. Heat Transfer Components in Open-End 2 Collector.

$$q_{gap\ 2} = \frac{1}{A_c} \frac{d_2^3 P C_p W g \sin\theta T_a}{12 R \nu} \frac{T_a}{T_p} \left(\frac{T_p}{T_a} - 1 \right) \qquad (33)$$

and the total heat transferred for geometry (4) can be found from equation (28).

RESULTS OF COOLING MODE ANALYSIS

Results of the heat transfer analyses explained in the previous sections are shown in Figures 7 through 15. Property values and collector dimensions used in the analysis are shown in Table I. Note that the ΔT's are generated by holding the ambient temperature constant at $24^{\circ}C$ and increasing the plate temperature. Curves for the open ended collector geometries terminate at low ΔT's under certain conditions due to a breakdown in the free convection analysis. This occurs if the cover temperature drops below ambient temperature to the point that the following condition is satisfied:

$$T_p - 2T_a + T_c = 0$$

At this combination of temperatures, $\dot{m}_1$ becomes zero and the flow would theoretically reverse direction. As noted, this condition is only satisfied at relatively low ΔT's and is considered out of the range of interest from a practical heat pump operation standpoint.

As can be seen from the graphs, the no-cover collector geometry is a superior heat dissipator under nearly all the conditions shown. The open end 2 geometry does out-perform the no-cover collector during combinations of low wind speeds, high effective sky temperatures, and fairly high ΔT's. The heat rejection ability of the open end 1 and closed cover collector geometry is limited except at high temperature differences.

The effect of wind speed and the effective sky temperature on the heat dissipation rate at a ΔT of $15^{\circ}C$ is shown in Figures 16 and 17, respectively. Note that only the no-cover geometry is significantly sensitive to either variable. However, since the effect of wind direction

TABLE I. Property Values and Dimensions Used in Cooling Mode Analysis Calculations.

(a) Collector Length = 2.5 meters

(b) Collector Width (W) = 1.0 meters

(c) Gap Distance (d) = 2.5 centimeters

(d) Tilt Angle (θ) = 45^{o}

(e) Atmospheric Pressure (P_a) = 1.013×10^{5} Kg/m^{3}

(f) Stefan-Boltzmann Constant (σ) = 5.6697×10^{-8} W/m^{2} K

(g) Gravitational Acceleration (g) = 9.807 m/sec^{2}

(h) Thermal Conductivity (k) = .0257 W/m K

(i) Specific Heat (C_p) = 1.005×10^{3} $\frac{J}{Kg\ K}$

(j) Collector Plate Emittance (ε_p) = 0.98

(k) Cover Emittance (ε_c) = 0.94

(l) Kinematic Viscosity (ν) = 1.55×10^{-5} m^{2}/sec

(m) Gas Constant for Air (R) = 287 $\frac{J}{Kg\ K}$

(n) Ambient Temperature (T_a) = $24^{o}C$

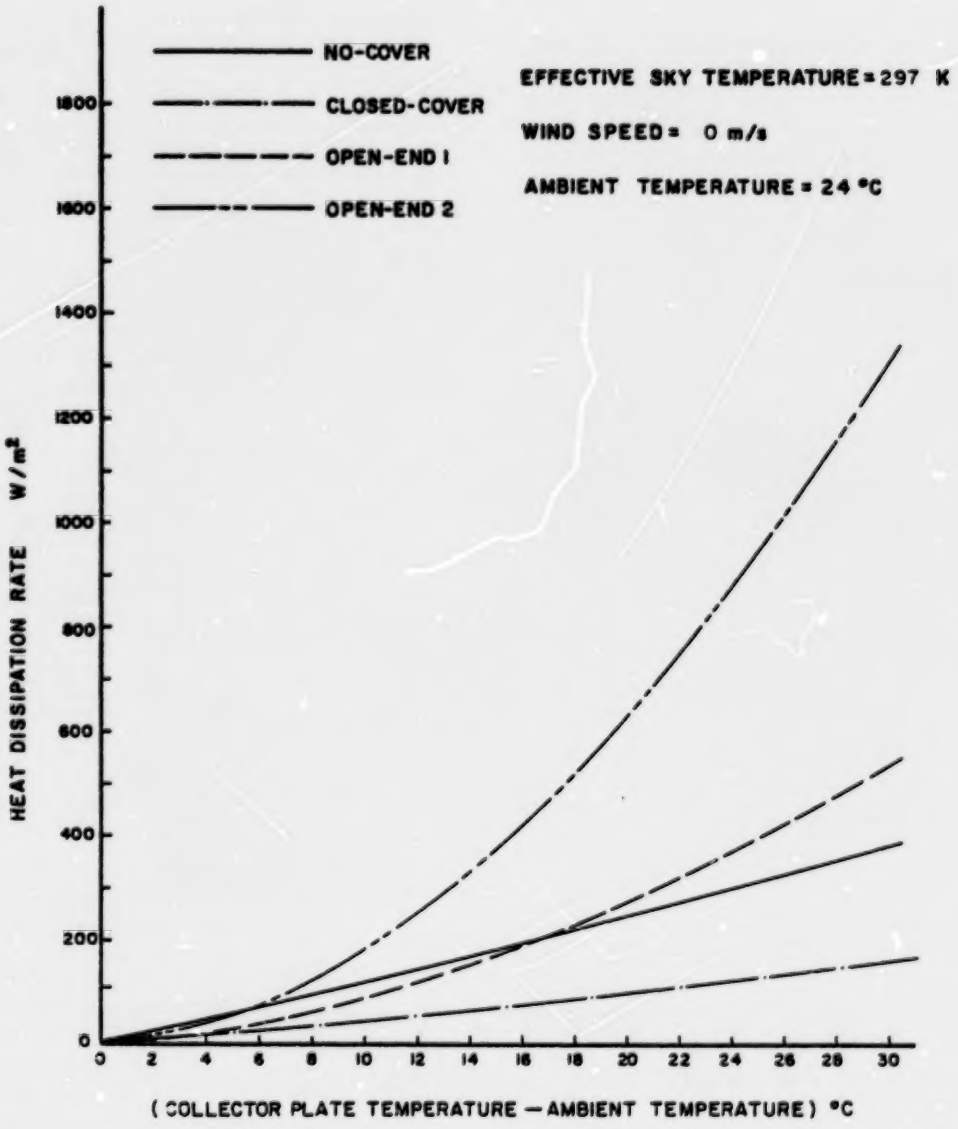

FIGURE 7. Nocturnal Heat Dissipating Ability as a Function of the Difference Between Collector Plate Temperature and Ambient Temperature.

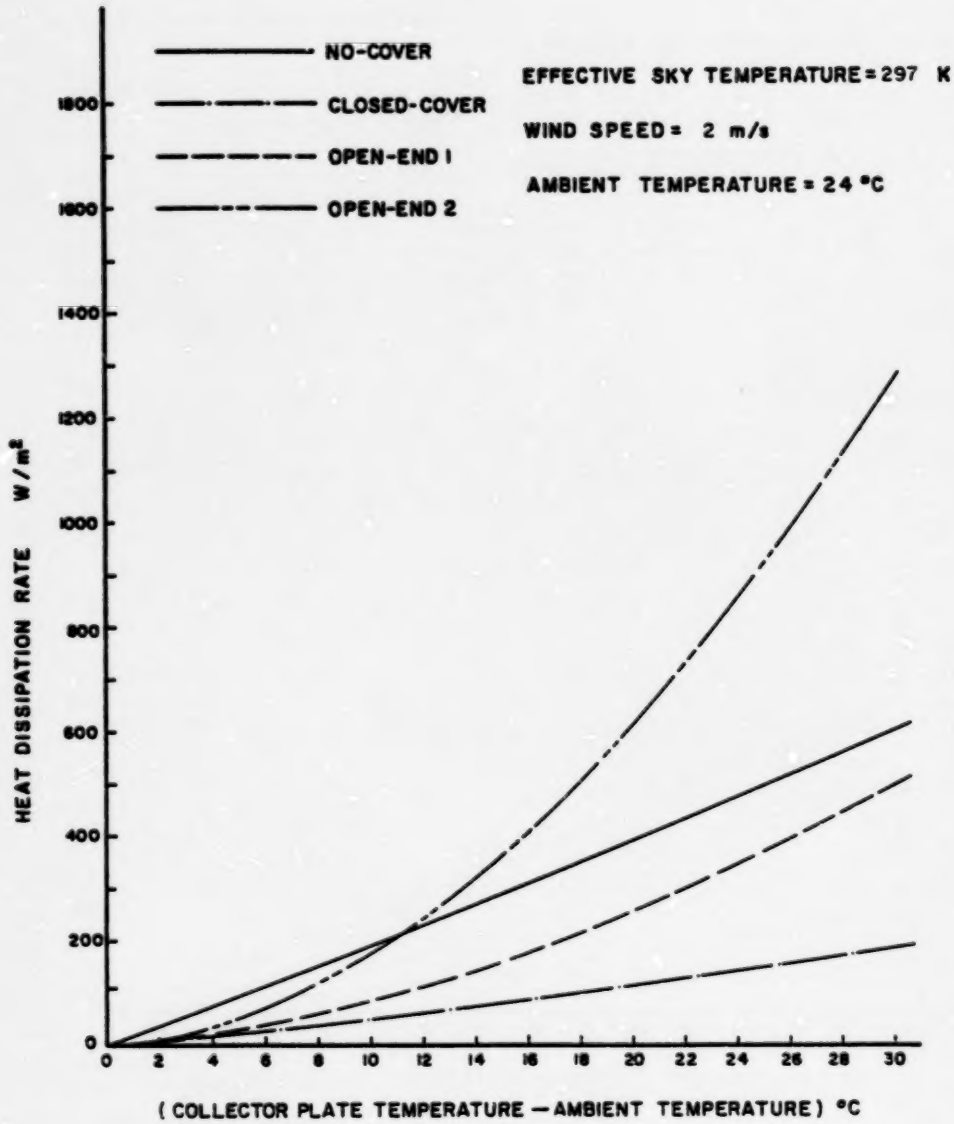

FIGURE 8. Nocturnal Heat Dissipating Ability as a Function of the Difference Between Collector Plate Temperature and Ambient Temperature.

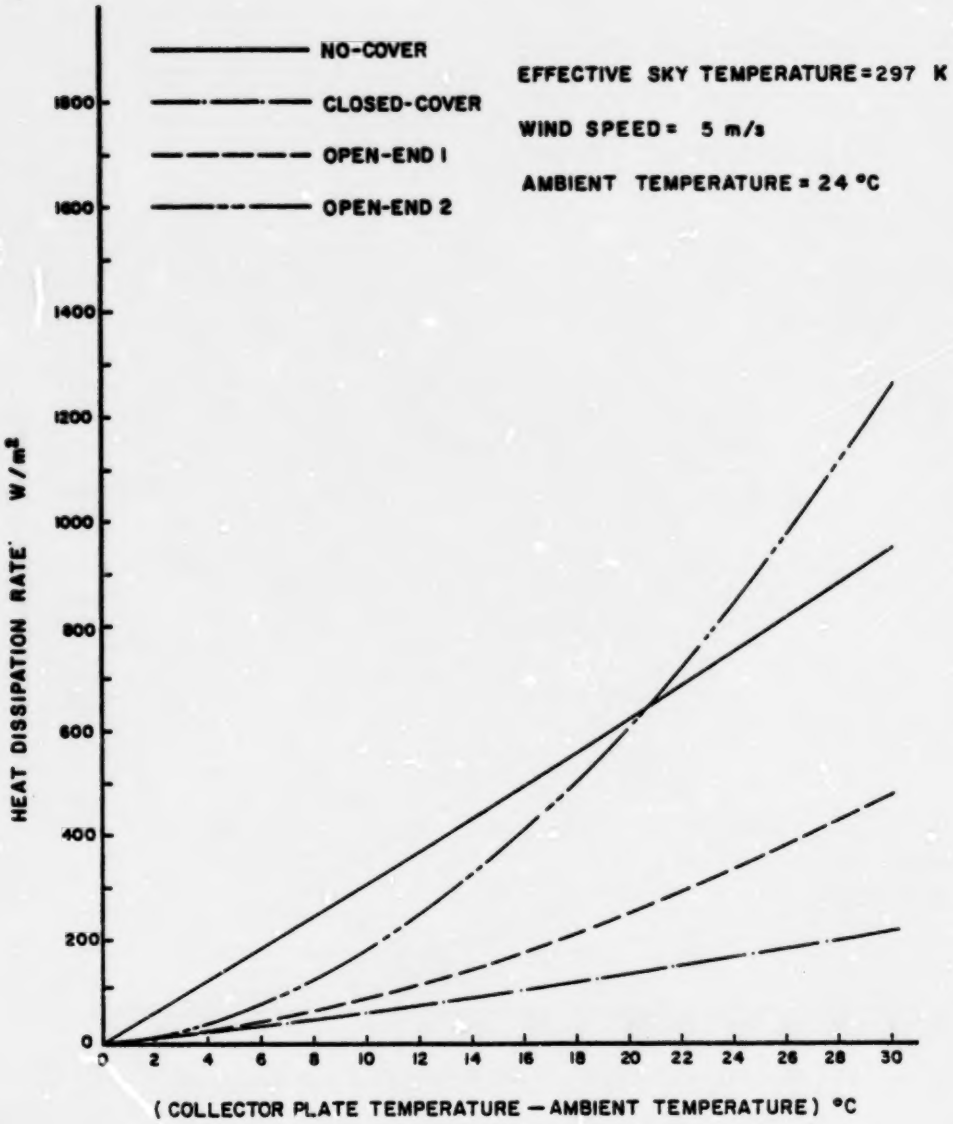

FIGURE 9. Nocturnal Heat Dissipating Ability as a Function of the Difference Between Collector Plate Temperature and Ambient Temperature.

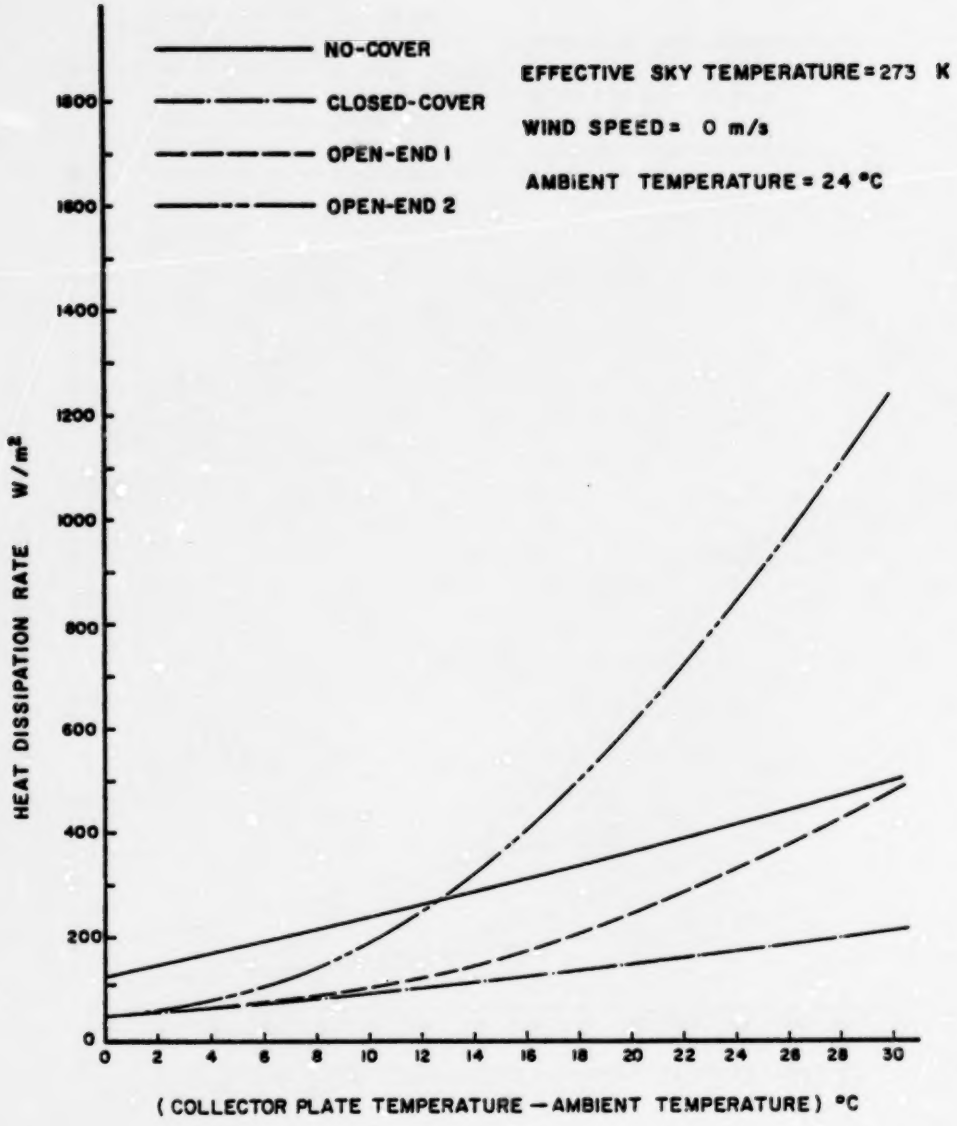

FIGURE 10. Nocturnal Heat Dissipating Ability as a Function of the Difference Between Collector Plate Temperature and Ambient Temperature.

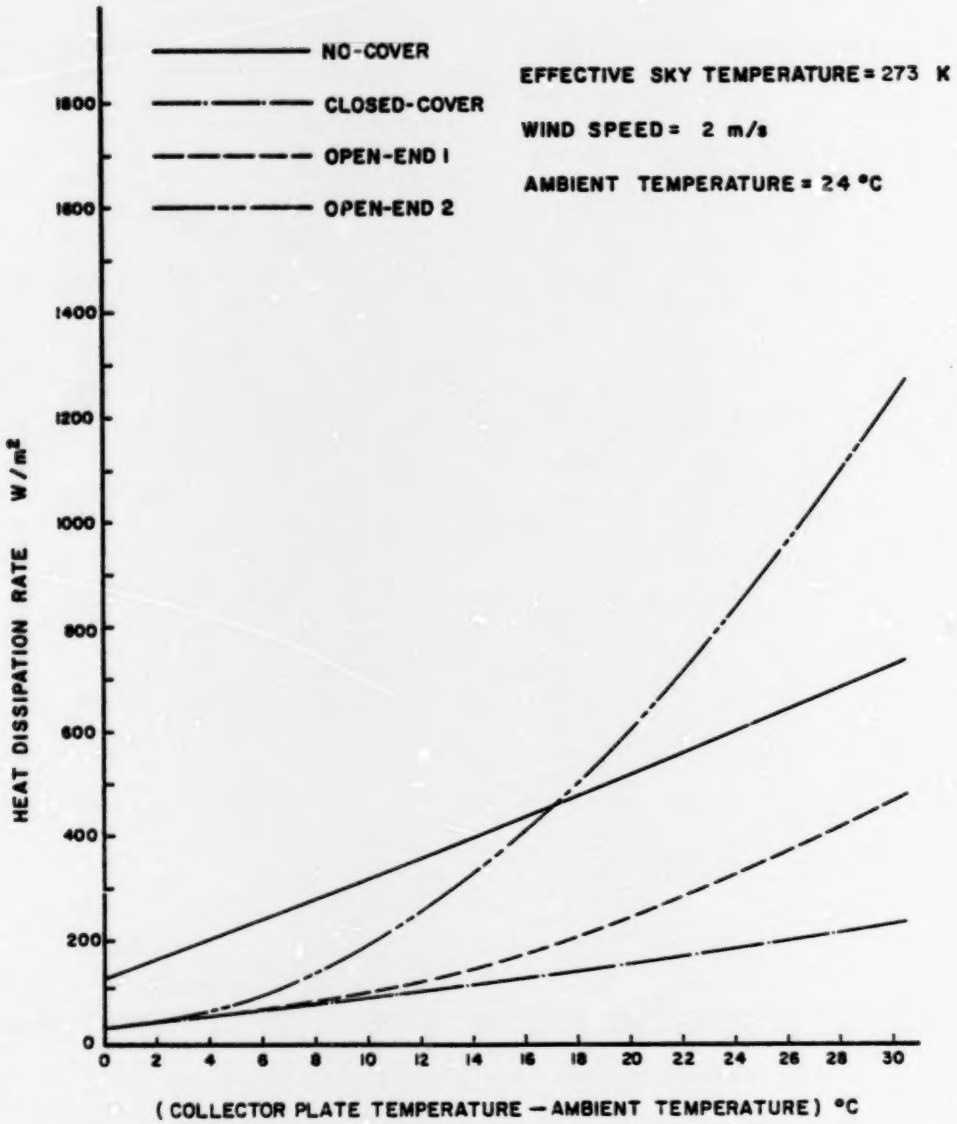

FIGURE 11. Nocturnal Heat Dissipating Ability as a Function of the Difference Between Collector Plate Temperature and Ambient Temperature.

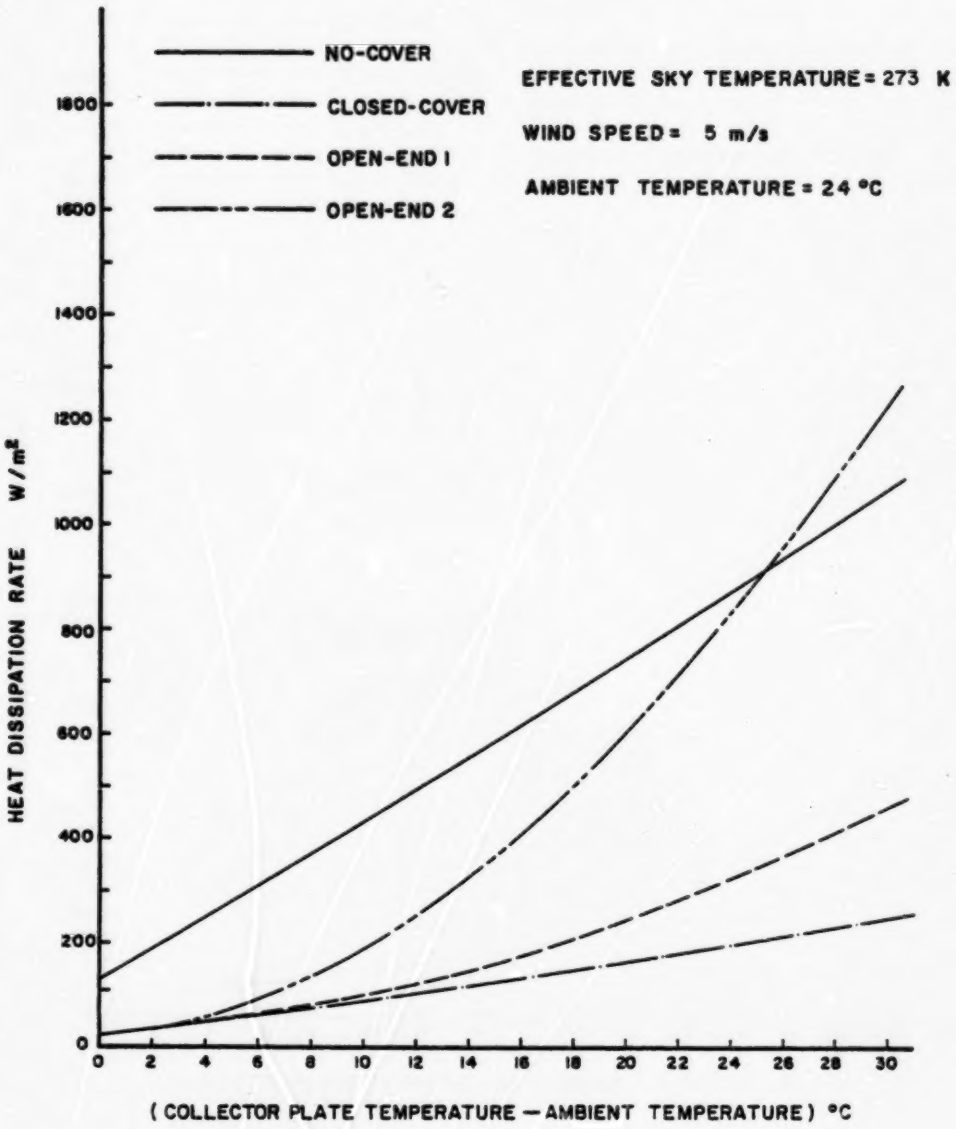

FIGURE 12. Nocturnal Heat Dissipating Ability as a Function of the Difference Between Collector Plate Temperature and Ambient Temperature.

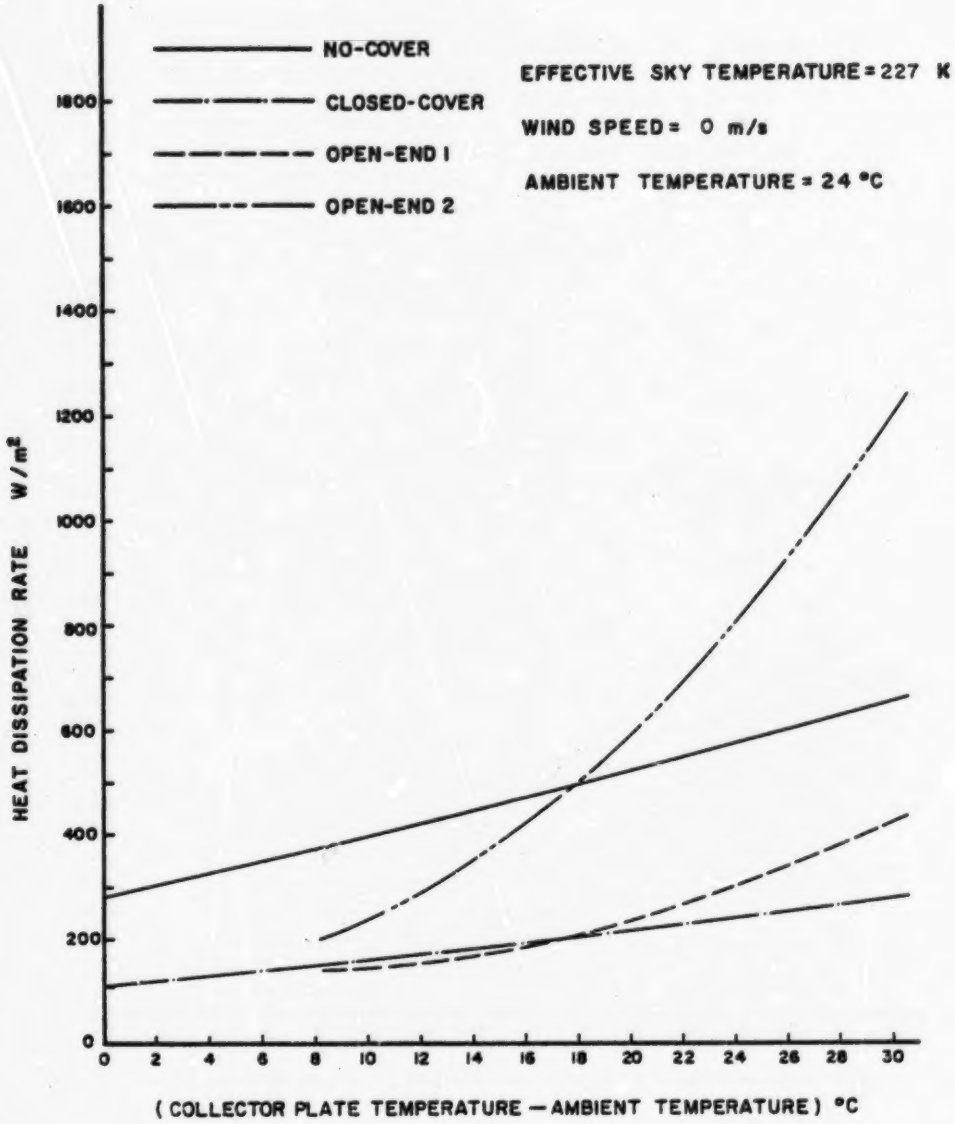

FIGURE 13. Nocturnal Heat Dissipating Ability as a Function of the Difference Between Collector Plate Temperature and Ambient Temperature.

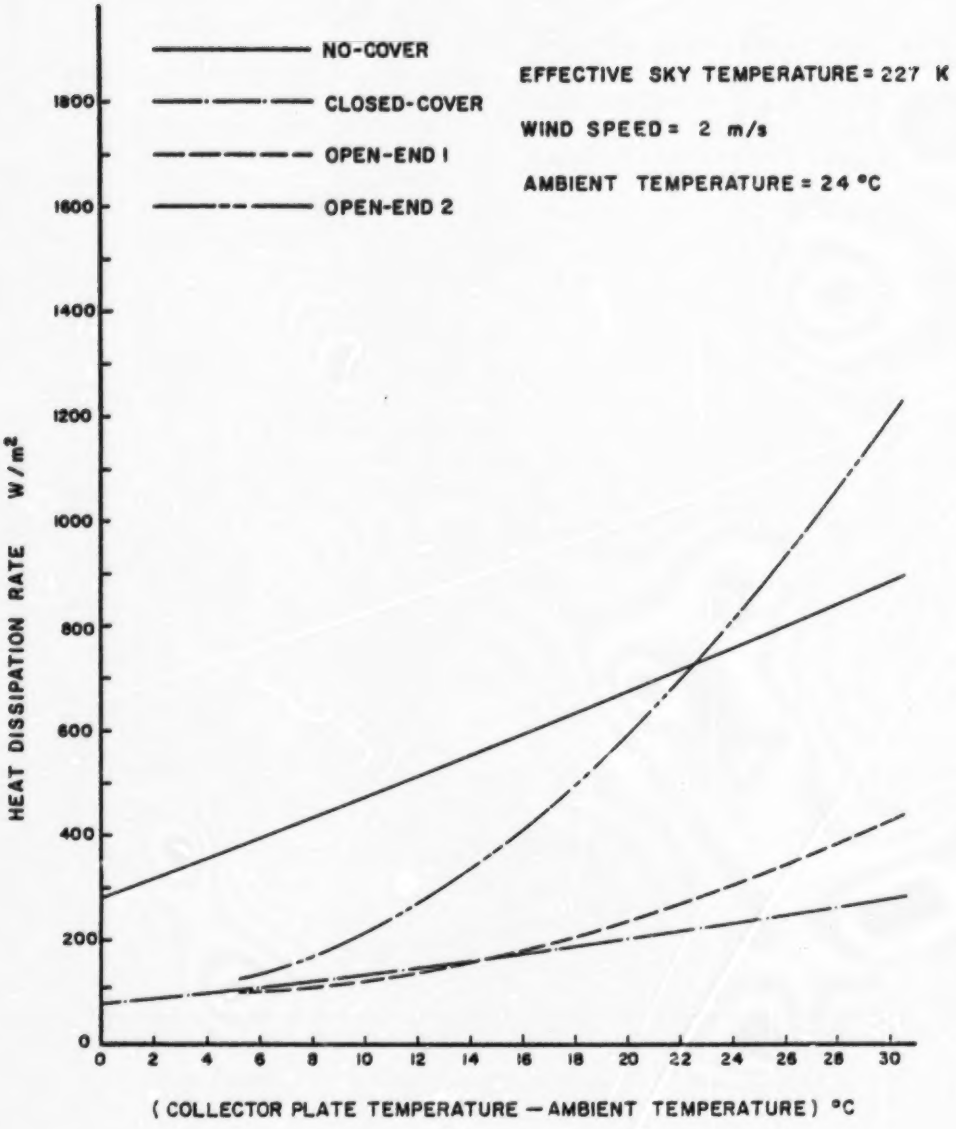

FIGURE 14. Nocturnal Heat Dissipating Ability as a Function of the Difference Between Collector Plate Temperature and Ambient Temperature.

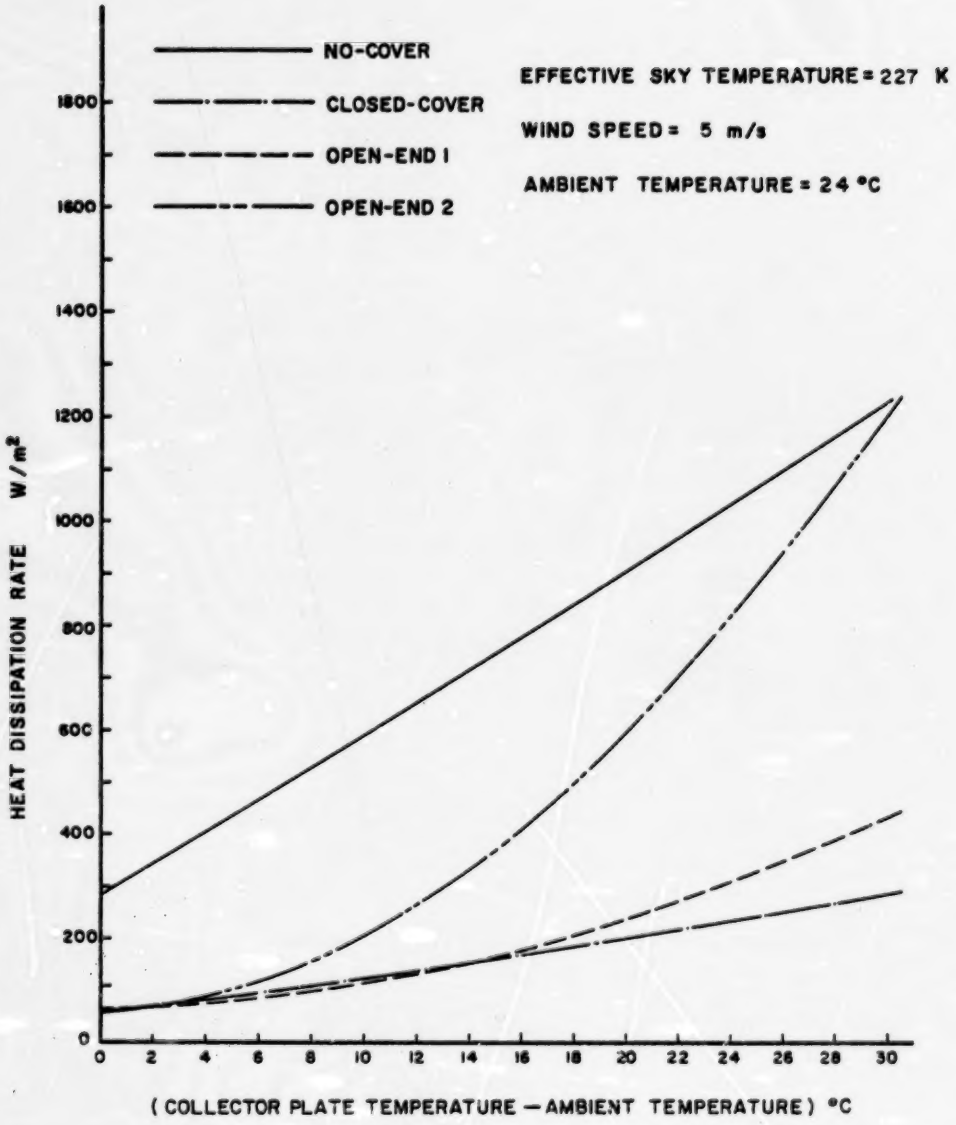

FIGURE 15. Nocturnal Heat Dissipating Ability as a Function of the Difference Between Collector Plate Temperature and Ambient Temperature.

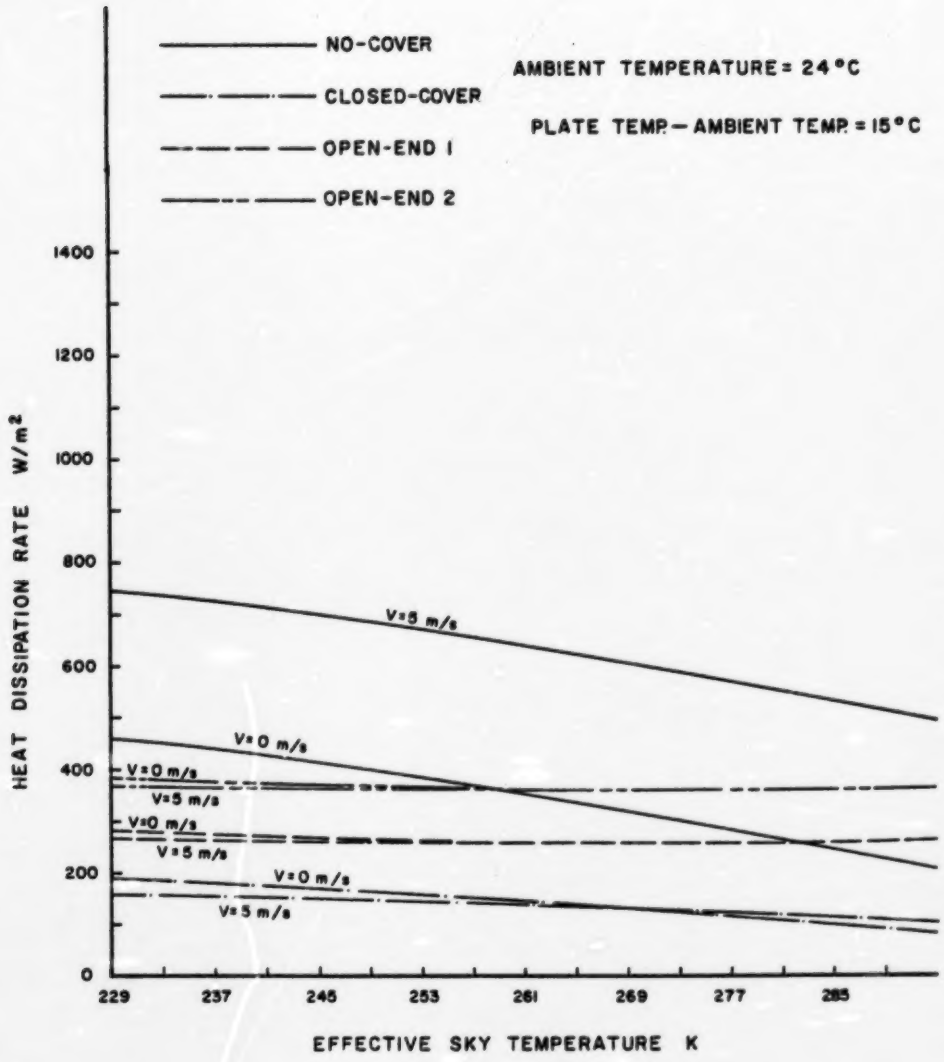

FIGURE 16. Nocturnal Heat Dissipating Ability as a Function of Effective Sky Temperature.

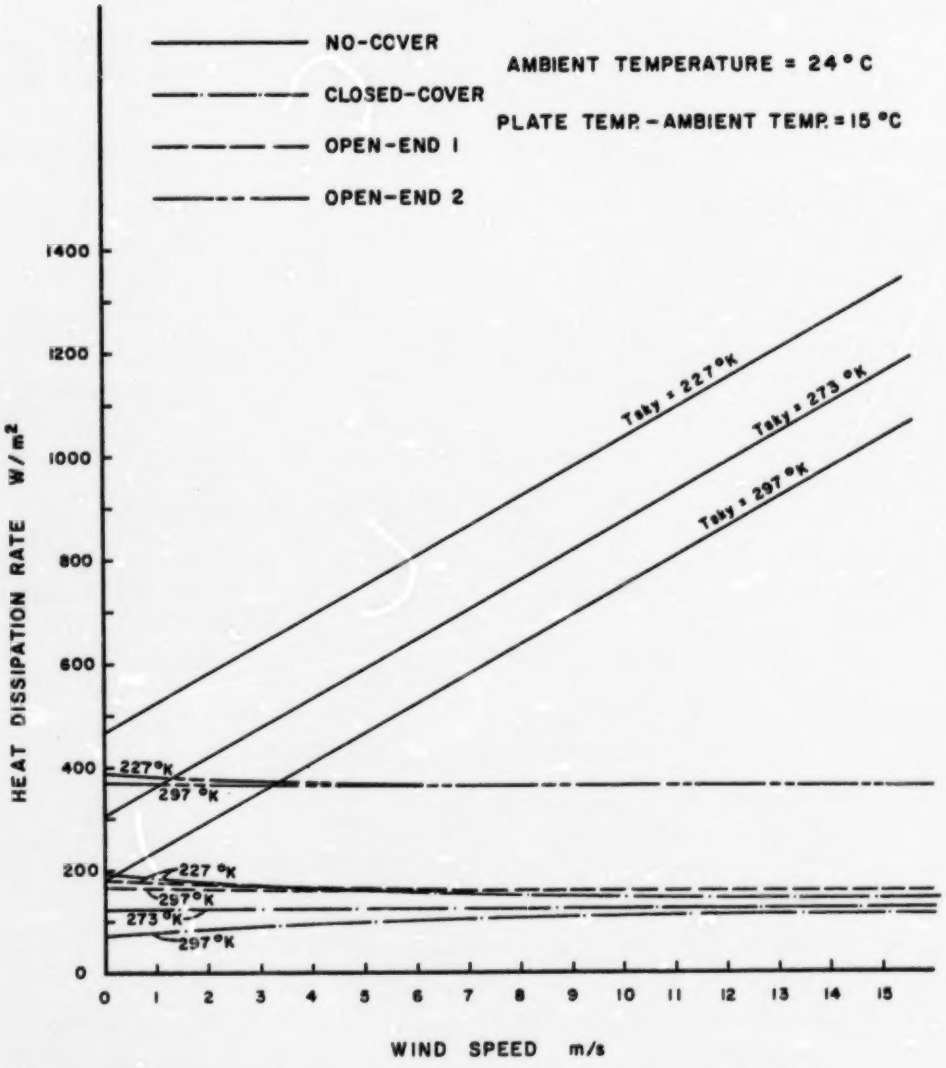

FIGURE 17. Nocturnal Heat Dissipating Ability as a Function of Wind Speed.

was not included in the analysis, the results shown above should be regarded with care. The free convection heat transfer component in the open-ended collector geometries would probably be enhanced by wind coming from most directions, although this relationship is not clearly established.

The selection of a particular collector geometry for use in a specific installation is influenced by the heating as well as cooling mode collector performance. Of course, the desired outcome is to utilize the collector system that will provide a high temperature heat source in winter and a low temperature heat sink in summer. Consideration must also be given to the demand requirements on the heat pump itself and the relative magnitude of loads as determined by the geographical location. For example, a structure in the North would have a relatively greater heating load and smaller cooling load than its counterpart in more southern regions. Additionally, heating mode collector efficiency is generally poorer in the North. Thus, an efficient winter absorber that may not necessarily be a good summer dissipator may be more cost effective in northern locations. In the South, on the other hand, a collector with no cover may provide adequate winter performance, while optimizing summer heat dissipating ability. These general conclusions are obviously affected by yearly heat pump operating costs versus initial collector cost considerations, and the choice of the most suitable option becomes quite involved and dependent on the characteristics of the specific application.

Heating mode performance for the no-cover and closed-cover collectors is shown in Figure 18 for a variety of operating conditions. The

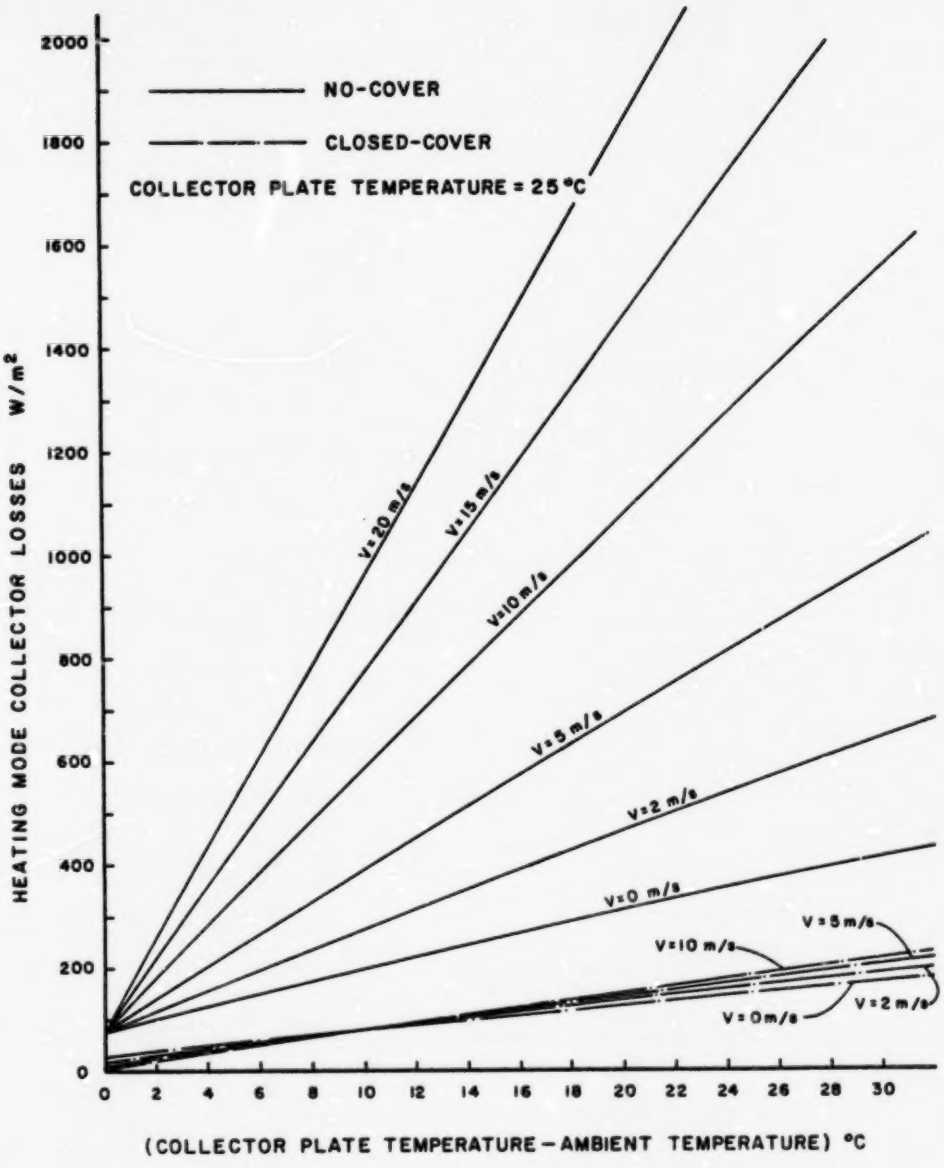

FIGURE 18. Heating Mode Collector Losses as a Function of the Difference Between Collector Plate Temperature and Ambient Temperature.

collector heat loss is plotted as a function of the difference between the collector plate temperature and the ambient temperature for various wind speeds. Note that for this case the ΔT is generated by holding the collector plate temperature constant while the ambient temperature is decreased. A collector plate temperature of $25^{\circ}C$ is considered in combination with wind speeds of 0, 2, 5, 10, 15, and 20 meters per second. Details of the heat transfer analysis for the heating mode operation are identical to the cooling mode analysis with the exception of the value of the effective sky temperature. Duffie and Beckman[1] suggest the use of the following relation given by Swinbeck (1963) for clear days:

$$T_s = 0.0552\ T_a^{1.5}$$

where T_s and T_a are in degrees Kelvin.

With the aid of the cooling and heating mode collector performance curves shown above, it is felt that the selection of the collector geometry most suitable for a specific application becomes clearer.

A brief outline of a simplified procedure for determination of the relative performance of the various collector options is given below. A mean daily solar insolation value for January is taken from U. S. Weather Bureau climatological data for Greensboro, North Carolina. It is assumed that the cooling load is equal to the heating load in one case and then equal to one-half the heating load in the second. The general approach taken is to size the collector area for the heating load and then determine the ΔT required to satisfy the heat dissipation rate necessary to meet the cooling load. Details of the analysis follow:

---

[1]See Reference 1, pg. 76.

Assumptions

(a) Solar insolation on a horizontal surface = 2.32 KWH/m^2-day

(b) Solar insolation on a surface tilted 45° = 3.55 KWH/m^2-day

(c) Heating load = 322 KWH/day

(d) Can collect heat over seven hour period

(e) Wind speed for heating and cooling modes = 2 m/sec

(f) Effective sky temperature for the cooling mode = 273 K

(g) The solar collector is operated in the heating mode at a ΔT of 15°C.

(h) Can dissipate heat over eight hour period

Calculations

(a) Heating load

First determine the average solar insolation for the seven hour heat collecting period. Thus,

Average solar heat available = 3.55/7 = 507 W/m^2

The heat loss under the conditions stated above can be found from Figure 41 for the no-cover and closed-cover geometries.

No cover heat loss = 335 W/m^2

Closed cover heat loss = 110 W/m^2

The heat collection ability of the two geometries is then found as follows:

No cover = 507 - 355 = 172 W/m^2

Closed cover = 507 - 110 = 397 W/m^2

Thus, the total collector area required is

No cover area = 32,200/(172)(7) = 267 m^2

Closed cover area = 32,200/(397)(7) = 116 m^2

(b) Cooling Load

(i) Case I - Cooling load = heating load = 322 KWH/day

For eight hour night must dissipate 332/8 = 40.2 KWH/hr

or

No-cover average heat dissipation rate =

$40,200/267 = 151\ W/m^2$

Closed-cover average heat dissipation rate =

$40,200/116 = 347\ W/m^2$

From Figure 34 the ΔT's required for the heat dissipation rates above are as follows:

No-cover - $1^{\circ}C\ \Delta T$

Closed-cover - off the graph

Closed-cover to open-end 1 = $25^{\circ}C\ \Delta T$

Closed-cover to open-end 2 - $14.5^{\circ}C\ \Delta T$

Note that is is assumed the no-cover collector remains as is, while the closed cover collector may be changed to either of the other geometries for cooling mode oepration.

(ii) Case II - Cooling load = one-half heating load = 161 KWH/day

The average heat dissipation rates are as follows:

No-cover collector = $75\ W/m^2$

Closed-cover collector = $173\ W/m^2$

Again, from Figure 34 the ΔT's are as follows:

No-cover - radiation alone is sufficient at $0^{\circ}C\ \Delta T$

Closed-cover - $23^{\circ}C\ \Delta T$

Closed-cover to open-end 1 - $16^{\circ}C\ \Delta T$

Closed-cover to open-end 2 - $10^{\circ}C\ \Delta T$

For optimum performance of the heat pump a small ΔT for both the heating and cooling modes is required. Both these objectives may be realized by increasing the collector area. However, this design option obviously leads to higher initial costs and the trade-off becomes one of increased initial cost versus higher operating costs. The matter is further complicated by the various collector alternatives, as can be seen even from the simplified analysis shown above.

While the selection of the most cost - effective collector alternative is a complex matter, the results of the preceding analysis do suggest the following general conclusions:

(1) It seems probable that for many applications the open-end 2 geometry presents a feasible means of utilizing the collector system as a heat sink without sacrificing heating mode performance or substantially adding to initial costs.

(2) Due to the severe heating mode losses suffered at even moderate wind speeds, it is felt that the no-cover collector would be practical only in applications where the cooling load exceeds the heating load and where high levels of solar insolation are available. This alternative would also seem the better choice if a lower heating mode coefficient of performance is acceptable.

(3) The open-end 1 and closed-cover collector geometries are unsuitable for use as heat dissipators.

In closing, it should be recognized that the results derived above are approximate and their principal importance is in presenting a performance comparison of the collector geometries considered. Absolute

values for the heat dissipation rates of the collectors under actual operating conditions must obviously be derived by experimental means. However, the conclusions drawn above do indicate that utilization of the collector system on a year-round basis is a practical means of justifying the high initial costs of a solar energy installation, particularly if the heat pump concept is employed.

CONCLUSION

The results of the present cooling mode analysis coupled with previously reported heat mode performance suggest that the solar assisted heat pump system is a viable alternative to the more conventional means of solar energy utilization. Thus, even though economic implications have not been fully explored, it is felt that construction of a larger scale prototype is certainly justified. The concluding remarks given here will therefore be limited to suggestions with regard to design considerations of such a system.

Since the response of the refrigerant flow control system is considered the most critical element in optimizing the performance of a solar assisted heat pump, it is recommended that externally driven compressors be specified for installation in a multiple compressor arrangement. This would allow maximum flexibility of control of the compressor displacement without requiring extensive modifications. Furthermore, the fine adjustment capability thus achieved would permit the establishment of optimum flow rates for various operating conditions and even allow for refrigerant substitutions. Additionally, most externally driven compressors are provided with a sight glass in the pump for monitoring the oil level, an important consideration in view of the difficulties encountered in the NCSU system. The use of compressors of this type would also have the benefit of the relative ease with which periodic inspections of the valves and piston rings could be made.

In conclusion, it is hoped that the material presented in this report will stimulate sufficient interest to encourage further research and development of solar assisted heat pumps. As noted earlier, the NCSU system was built on a limited budget and was undertaken primarily as a design exercise for undergraduate engineering students. Therefore, significant performance improvement is considered possible.

BIBLIOGRAPHY

1. Duffie, J. A. and Beckman, W. A. Solar Energy Thermal Processes, John Wiley and Sons, New York, 1974.

2. Hackforth, H. L. Infrared Radiation, McGraw-Hill, New York, 1960, pp. 42-45.

3. White, F. M. Viscous Fluid Flow, McGraw-Hill, New York, 1974.

APPENDIX

OPEN-ENDED COLLECTORS HEAT TRANSFER ANALYSIS

A. Open-End 1 Collector

For sake of clarity, the heat transfer components involved in the open-end 1 collector geometry are shown in Figure 19. Treatment of the radiation components, $q_{r,p-c}$ and $q_{r,c-s}$, and the convection components, $q_{c,p-c}$ and $q_{c,c-s}$, is given in the cooling analysis. Therefore, consideration here is limited to the development of the natural convection draft problem.

As mentioned in the cooling mode analysis, air at ambient temperature (T_a) enters the opening at the bottom of the collector, is heated by the warm plate and exits through the top opening. The net energy transferred from the plate to the air ($Q_{gap\ 1}$) is a function of the air mass flow rate and the bulk fluid temperature[1] (T_{01}) at the exit. That is,

$$Q_{gap\ 1} = \dot{m}_1\, C_p (T_{01} - T_a) \qquad (A.1)$$

It is assumed that the flow is essentially incompressible and that fully developed laminar flow exists at the exit. Thus,

$$u = u(y) \quad \text{only}$$

and

$$T = T(y) \quad \text{only}$$

The bulk fluid temperature is defined as:

---

[1] Also known as mixed mean fluid temperature.

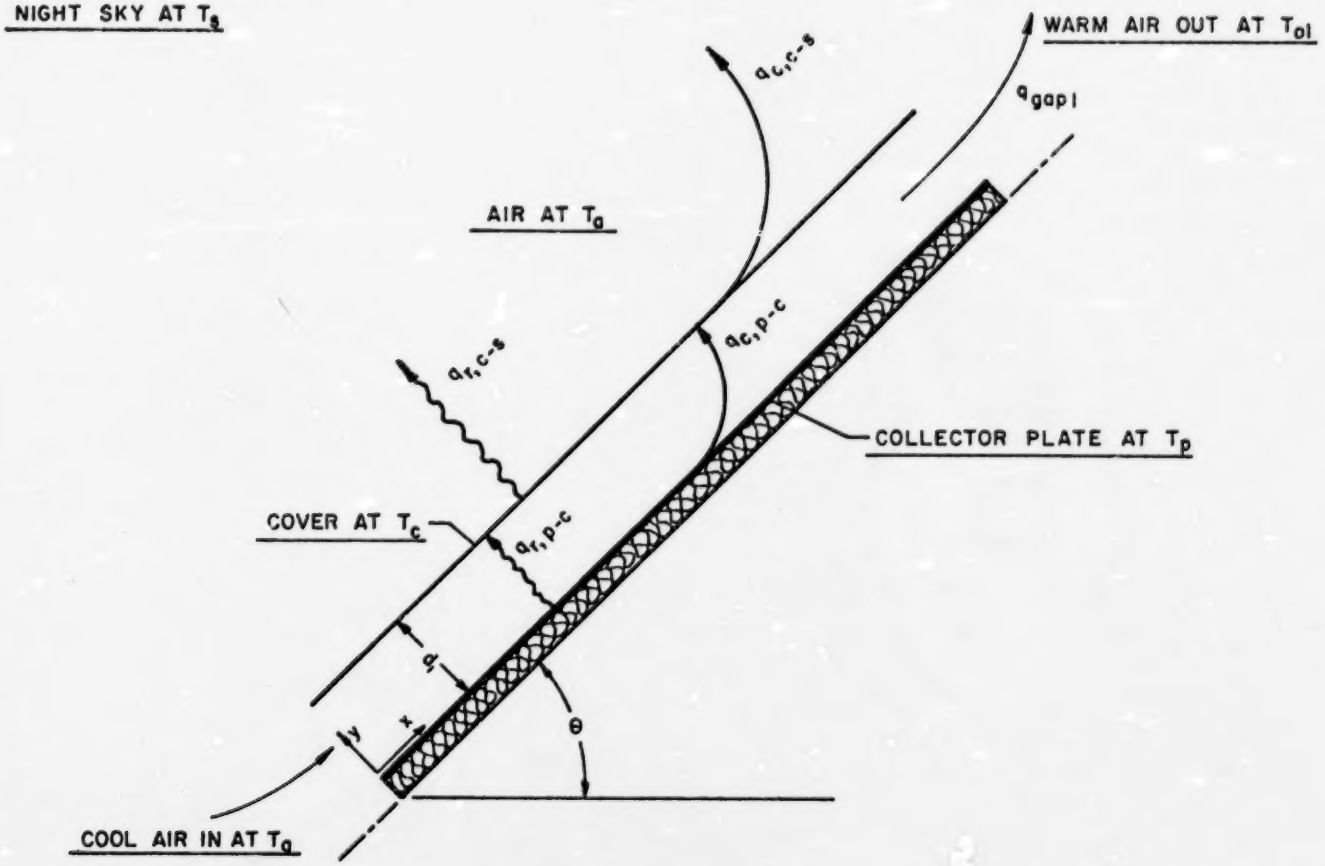

FIGURE 19. Heat Transfer Components in Open-End 1 Collector.

$$T_{01} = \frac{\int_0^d u(y)\, T(y)\, dy}{\int_0^d u(y)\, dy} \tag{A.2}$$

and the mass flow is defined in terms of the mean fluid velocity $\bar{u}$ as

$$\dot{m}_1 = \rho_o A_{gap} \bar{u} \tag{A.3}$$

where

$$\bar{u} = \frac{1}{d} \int_0^d u(y)\, dy \tag{A.4}$$

and

$$A_{gap} = dW \tag{A.5}$$

As can be seen from the relations shown above, determination of $Q_{gap\ 1}$ requires the solution of the governing flow equations for the temperature and velocity profiles. The governing equations are as follow:

(a) Continuity Equation

$$\frac{\partial u}{\partial x} + \frac{\partial v}{\partial y} = 0 \tag{A.6}$$

(b) X-Momentum Equation

$$\rho\left(u \frac{\partial u}{\partial x} + v \frac{\partial u}{\partial y}\right) = - \frac{\partial P}{\partial x} - \rho\, g_x + \mu \frac{\partial^2 u}{\partial y^2} \tag{A.7}$$

(c) Energy Equation

$$u \frac{\partial T}{\partial x} + v \frac{\partial T}{\partial y} = \alpha \frac{\partial^2 T}{\partial y^2} \tag{A.8}$$

Since the flow is generated by thermal effects, the equations are coupled and the solution for the velocity profile requires knowledge of

the temperature distribution. Consider the energy equation. If it assumed that the temperature profile is essentially constant in the region near the exit[2] the analysis is greatly simplified and the energy equation reduces to an ordinary differential equation. The boundary conditions are constant wall temperatures, T_p at the plate and T_c at the cover. Thus, $\partial T/\partial x \simeq 0$, $v = 0$ for fully developed flow and constant profiles and

$$T = T_p \text{ @ } y = 0$$

$$T = T_c \text{ @ } y = d$$

Therefore,

$$\frac{\partial^2 T}{\partial y^2} = 0 \tag{A.9}$$

Integrating

$$\frac{\partial T}{\partial y} = C_1 \tag{A.10}$$

and

$$T = C_{1y} + C_2 \tag{A.11}$$

but

$$T = T_p \text{ @ } y = 0$$

and

$$T = T_c \text{ @ } y = d$$

Thus,

$$T_{g1} = \frac{y}{d} (T_c - T_p) + T_p \tag{A.12}$$

---

[2]See Reference 3, pp. 114-117.

Note the resulting temperature profile is linear in y. Next consider the continuity and x-momentum equations. Since the flow is fully developed (v = 0), the continuity equation yields the following result:

$$\frac{\partial u}{\partial x} = 0 \tag{A.13}$$

Thus, the x-momentum equation becomes

$$0 = - \frac{\partial P}{\partial x} - \rho\, g_x + \mu \frac{\partial^2 u}{\partial y^2} \tag{A.14}$$

where $- \rho\, g_x$ = the body force in the x-direction.

The pressure force term under these conditions is the external "hydrostatic" pressure gradient due to changes in elevation. Thus,

$$\frac{\partial P}{\partial x} = - \rho_a\, g_x \tag{A.15}$$

Substitution into equation (2.12) yields

$$0 = g_x(\rho_a - \rho) + \mu \frac{\partial^2 u}{\partial y^2} \tag{A.16}$$

The density difference $(\rho_a - \rho)$ may be approximated in terms of the volume coefficient of expansion, as follows:

$$\beta = \frac{1}{V} \left(\frac{\partial V}{\partial T}\right)_p = \frac{1}{V_a} \frac{V - V_a}{T - T_a} \tag{A.17}$$

or

$$\beta = \frac{\rho_a - \rho}{\rho(T - T_a)} \tag{A.18}$$

Thus,

$$(\rho_a - \rho) = \rho(T - T_a)\beta \tag{A.19}$$

Substitution of equation (A.17) into equation (A.14) and dividing by ρ yields,

$$0 = g_x \beta(T - T_a) + \nu \frac{\partial^2 u}{\partial y^2} \qquad (A.20)$$

But, $g_x = g \sin \theta$ for the geometry given and $T = \frac{y}{d} (T_c - T_p)$ from the equation (A.10). Thus, after rearranging, the x-momentum equation becomes

$$\frac{\partial^2 u}{\partial y^2} = - \frac{\beta g \sin \theta}{\nu} \left[\frac{y}{\delta} (T_c - T_p) + T_p - T_a\right] \qquad (A.21)$$

The no slip boundary conditions are

$$\begin{aligned} u &= 0 \ @ \ y = 0 \\ u &= 0 \ @ \ y = d \end{aligned} \qquad (A.22)$$

Integrating equation (2.19) twice yields

$$u_1 = - \frac{\beta g \sin \theta}{\nu} \left[\frac{y^3}{6d} (T_c - T_p) + \frac{y^2}{2} (T_p - T_a)\right] + C_{1y} + C_2 \qquad (A.23)$$

Application of the boundary conditions results in the following

$$C_1 = \frac{\beta g \sin \theta}{\nu} \left[\frac{d}{6} (T_c - T_p) + \frac{d}{2} (T_p - T_a)\right] \qquad (A.24)$$

and

$$C_2 = 0$$

So the velocity profile becomes

$$u_1 = \frac{\beta g \sin \theta}{\nu} \{(T_c - T_p) \left(\frac{yd}{6} - \frac{y^3}{6d}\right) + (T_p - T_a) \left(\frac{yd}{2} - \frac{y^2}{2}\right)\} \qquad (A.25)$$

If the air is considered an ideal gas the volume coefficient of expansion may be expressed as follows

$$\beta = \frac{\frac{\rho_a}{\rho} - 1}{(T - T_a)}$$

from equation (A.16) and

$$\rho = \frac{P}{RT}$$

from the ideal gas law. So

$$\beta = \frac{\frac{T}{T_a} - 1}{T - T_a} = \frac{\frac{T}{T_a} - 1}{T_a \left(\frac{T}{T_a} - 1\right)}$$

or

$$\beta = \frac{1}{T_a} \tag{A.26}$$

With a knowledge of the approximate velocity and temperature profiles derived above the solution for the bulk fluid temperature and the mass flow rate may be carried out by substituting the appropriate functions in equations (A.2), (A.3), and (A.4). Performing the necessary integrations results in the following expressions

$$T_{01} = \frac{\frac{8}{15}(T_p + T_c)^2 - T_a(T_p + T_c) - \frac{2}{15} T_p T_c}{T_p - 2 T_a + T_c} \tag{A.27}$$

$$\bar{u}_1 = \frac{d^2 \beta g \sin \theta}{24 \nu} (T_p - 2 T_a + T_c) \tag{A.28}$$

and

$$\dot{m}_1 = \frac{\rho_o W d^3 \beta g \sin \theta}{24 \nu T_a} (T_p - 2 T_a + T_c) \tag{A.29}$$

where ρ_o is the density evaluated at the bulk fluid temperature which can be expressed with the use of the perfect gas law as follows

$$\rho_o = \frac{P_a}{R T_{01}} \tag{A.30}$$

where P_a is the atmospheric pressure, assumed constant. Thus, after substituting for β from equation (A.26), the flow rate becomes

$$\dot{m}_1 = \frac{P_a W d^3 g \sin\theta}{R T_{01} 24 \nu T_a} (T_p - 2 T_a + T_c) \qquad (A.31)$$

and the net energy absorbed by the air in flowing through the collector is given by equation (A.1). For a collector of characteristic dimensions, the average heat transferred per unit area may be found by dividing by the collector area. Thus

$$q_{gap\ 1} = \frac{1}{A_c} (\dot{m}_1)(C_p)(T_{01} - T_a) \qquad (A.32)$$

Note that the subscript 1 refers to the gap above the collector plate.

B. Open-End 2 Collector

As in the previous section, the discussion here is limited to the convection problem through the air gap. The principal heat transfer components are shown in Figure 20. Since it is assumed that the collector plate temperature is held constant, the heat transfer components above the plate are unaffected by the convection through the lower air gap. Therefore, consideration here is given only to the development of the free convection below the collector plate. Again it is assumed the flow is fully developed, laminar and essentially incompressible in the region near the exit. The constant profile assumption is also required for simplification. Thus, the governing equations reduce to the following

(a) Continuity

$$\frac{\partial u}{\partial x} = 0 \qquad (A.33)$$

(b) X-Momentum

$$\frac{\partial^2 u}{\partial y^2} = \frac{\beta g \sin\theta}{\nu} (T_a - T) \qquad (A.34)$$

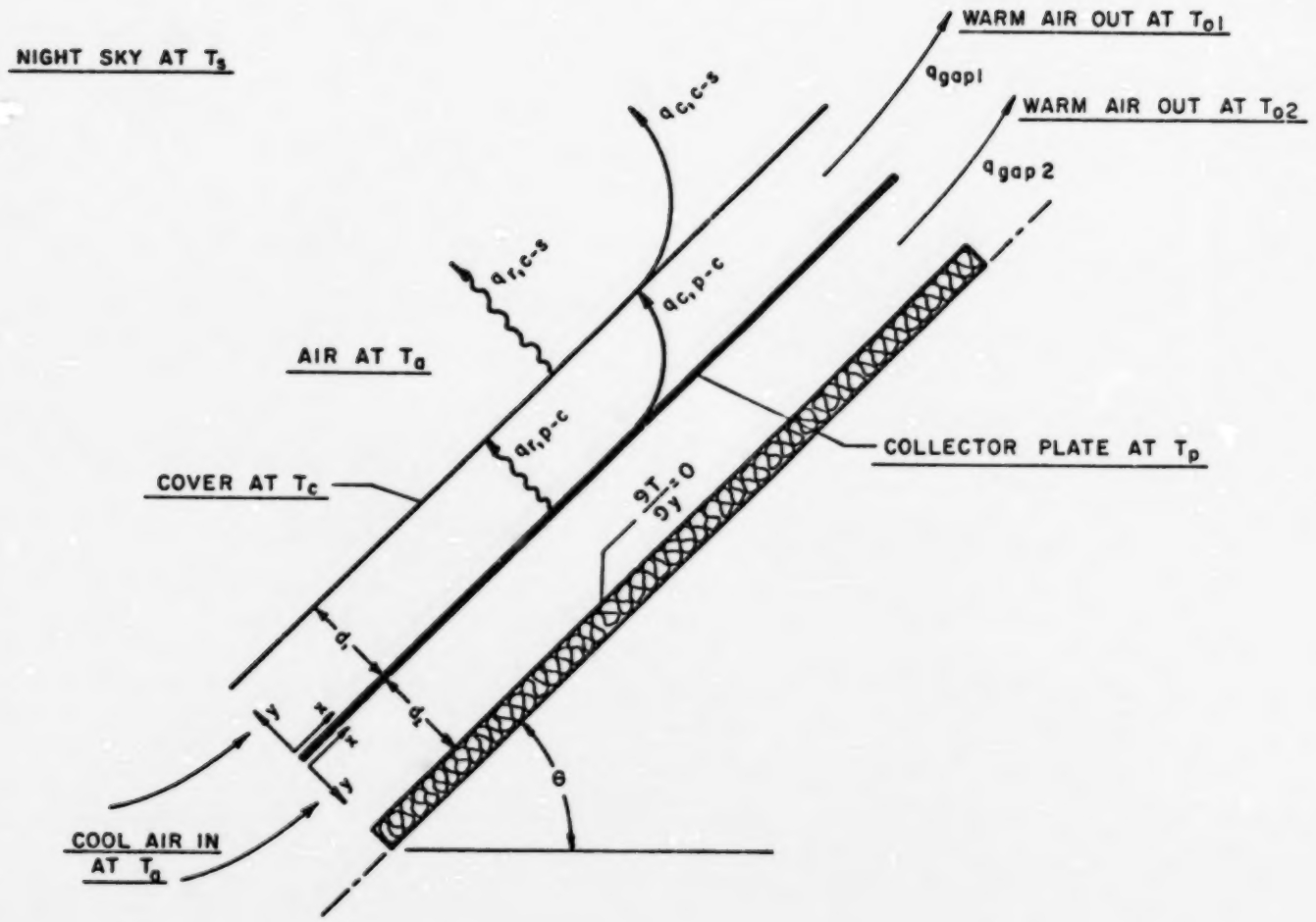

FIGURE 20. Heat Transfer Components in Open-End 2 Collector.

(c) Energy Equation

$$\frac{\partial^2 T}{\partial y^2} = 0 \tag{A.35}$$

Note the equations are coupled as before, and the solution first requires determination of the temperature profile. The appropriate boundary conditions are as follows

$$T = T_p \text{ @ } y = 0$$

$$\frac{\partial T}{\partial y} = 0 \text{ @ } y = d_2 \tag{A.36}$$

Thus

$$T_{g2} = C_{1y} + C_2$$

and

$$C_1 = 0 \quad , \quad C_2 = T_p$$

so

$$T_{g2} = T_p \tag{A.37}$$

Note the temperature is constant all across the air gap and the bulk fluid temperature T_{02} is equal to the plate temperature of

$$T_{02} = T_p \tag{A.39}$$

Substitution of equation (A.37) into the x-momentum equation yields the following

$$\frac{\partial^2 u}{\partial y^2} = \frac{\beta g \sin \theta}{\nu} [T_a - T_p] \tag{A.40}$$

But

$$\beta = \frac{1}{T_a}$$

So

$$\frac{\partial^2 u}{\partial y^2} = \frac{g \sin\theta}{\nu}\left[1 - \frac{T_p}{T_a}\right] \tag{A.41}$$

and after integrating

$$u = \frac{g \sin\theta}{2\nu}\left[1 - \frac{T_p}{T_a}\right] y^2 + C_1 y + C_2 \tag{A.42}$$

The no slip boundary conditions are

$$u = 0 \text{ @ } y = 0$$

$$u = 0 \text{ @ } y = d_2$$

Thus

$$u_2 = \frac{g \sin\theta}{2\nu}\left(1 - \frac{T_p}{T_a}\right)(y^2 - d_2 y) \tag{A.43}$$

Substitution of these profiles into the expressions for $\bar{u}$ and $\dot{m}$ yields

$$\bar{u}_2 = \frac{d_2^2 g \sin\theta}{12\nu}\left(\frac{T_p}{T_a} - 1\right) \tag{A.44}$$

$$\rho_o = \frac{P_a}{R T_p} \tag{A.45}$$

$$\dot{m}_2 = \frac{P_a d_2^3 W g \sin\theta}{12 R \nu}\left(\frac{1}{T_a} - \frac{1}{T_p}\right) \tag{A.46}$$

Thus, the net energy absorbed by the air flowing through the lower gap, on a unit collector area basis, is given by

$$q_{gap\ 2} = \frac{d_2^3 P_a C_p W g \sin\theta}{A_c\ 12 R \nu}\frac{T_a}{T_p}\left[\frac{T_p}{T_a} - 1\right] \tag{A.47}$$

1. Report No.	2. Government Accession No.	3. Recipient's Catalog No.
NASA CR-3111		

4. Title and Subtitle	5. Report Date
An Analytical Investigation of the Performance of Solar Collectors as Nighttime Heat Radiators in Airconditioning Cycles	March 1979
	6. Performing Organization Code

7. Author(s)	8. Performing Organization Report No.
Clay B. Jones and Frederick O. Smetana	
	10. Work Unit No.

9. Performing Organization Name and Address	11. Contract or Grant No.
North Carolina Science and Technology Research Center, P.O. Box 12235, Research Triangle Park, NC 27709	Outgrowth of NAS1-14208
	13. Type of Report and Period Covered

12. Sponsoring Agency Name and Address	13. Type of Report and Period Covered
National Aeronautics and Space Administration Washington, DC 20546	Contractor Report
	14. Sponsoring Agency Code

15. Supplementary Notes

Langley Technical Monitor: John Samos

16. Abstract

An analytical investigation was carried out to determine the ability of typical solar collectors to serve as nighttime heat radiators. Such use might be made of the collectors during the summertime where they then serve as the condenser in a heat pump cycle with electrically-driven mechanical compressor. In winter the collectors form a solar-heated evaporator in the heat pump cycle. It was found that if one opens the upper and lower ends of a collector, large free convection currents may be set up between the collector surface and the cover glass(es) which can result in appreciable heat rejection. If the collector is so designed that both plate surfaces are exposed to convection currents when the upper and lower ends of the collector enclosure are opened, the heat rejection rate is 300 watts/m^2 when the plate is 13^{o} C above ambient. This is sufficient to permit a collector array designed to provide 100% of the heating needs of a home to reject the accumulated daily air conditioning load during the course of a summer night. This also permits the overall energy requirement for cooling to be reduced by at least 15% and shift the load on the utility entirely to the nighttime hours.

17. Key Words (Suggested by Author(s))	18. Distribution Statement
Solar Energy Nighttime Heat Radiators	Unclassified - Unlimited Subject Category 44

19. Security Classif. (of this report)	20. Security Classif. (of this page)	21. No. of Pages	22. Price*
Unclassified	Unclassified	60	$5.25

* For sale by the National Technical Information Service, Springfield, Virginia 22161

NASA-Langley, 1979